Report No. 120

LAMINAR MIXING OF A SUSPENSION WITH A CLEAN STREAM

by

Bernard Otterman

and

Shao-lin Lee

September 1968

LAMINAR MIXING OF A SUSPENSION WITH A CLEAN STREAM

by

Bernard Otterman
Assistant Professor
Department of Mechanical Engineering
Northeastern University

and

Shao-lin Lee
Professor
Department of Mechanics
State University of New York at Stony Brook

Report No. 120
September 1968

Abstract

From a review of single particle behavior, it was concluded that both drag and slip-shear forces determine the interaction between the phases. Treating the particulate phase as a continuum, the basic conservation equations were non-dimensionalized in terms of the particle slip relaxation time and/or slip relaxation distance. This resulted in identification of a dimensionless constant to which the slip-shear effects are proportional, and yielded a set of "universal" two phase boundary layer equations applicable to a class of particulate suspensions. These in turn were solved for the case of laminar mixing of a suspension stream with a clean fluid stream. From perturbation solutions valid in the initial portion of the mixing layer and in the far down stream regions, a description of the velocity field of both phases, the slip between the phases, and the particulate concentration within the mixing layer was obtained. It was shown that mixing of the particulate phase with the clean fluid is entirely due to the effects of the slip-shear forces. However, that particle injection into the clean fluid occurs only within the initial portion of the mixing layer. In this region particles exhibit two directional migration characteristics. In the far out mixing region the particulate phase is essentially frozen to the local fluid, with the slip shear forces again determining the particulate concentrations within the mixing layer. The results correlate with hereto unexplained experimental observations, and consequently contribute to a more accurate understanding of particle migration phenomena in laminar suspension flows.

I. Introduction

The behavior of multiphase systems which are characterized by the motion of aggregates of small solid particles and/or liquid drops relative to fluids in which they are suspended covers a wide range of phenomena of great technical importance. Many examples [18] can be cited, including the collection of dust and mist from chemical processes in order to reduce or eliminate atmospheric pollution. Recently, however, as a result of the pioneering work of Marble (1964) [11], Singleton (1965) [17], and Soo (1967) [18] and others [2, 3, 9] the fluid mechanics of multiphase systems has been separated from particular detailed problems and has found a place in the general discipline of fluid mechanics. Our aim is to contribute further to this effort by investigating the role of slip-shear forces in laminar boundary layer suspension flows. In particular we are interested in gaining a better understanding of the experimentally observed, Young (1960) [21], Segre and Silberberg (1962) [15], and Karmis et al (1966) [6], but hereto unexplained particle migration in laminar suspension flows. In the case of tube flows, the migration resulted in accumulation of particles near the wall [21], or on the axis with a particle free zone near the wall [6], or in an annular region between the tube wall and axis [15]. A comprehensive review of lateral migration characteristics in tubes is given by Brenner (1966) [1] and Lawler and Lu (1967) [8]. The latter also treat the problem of particle migration in rotating tubes. The general feature of this migration is the movement of particles across fluid stream lines in regions where there exists a fluid shear. Moreover, as was pointed out in [12] and [14], in the absence of centrifugal forces, particle migration is probably due to

an interaction of the particle with the walls which is inertial in nature, in combination with slip-shear effects. Because very little is known concerning the former, even in the case of a single particle, we have selected a flow situation which is of significant practical importance, but in which the drag and slip-shear effects entirely determine the migration characteristics, i.e., laminar mixing of a suspension with a clean fluid.

Up to now, a theoretical or experimental study of this problem has not been reported in the open literature. Soo (1965) [19] investigated the laminar mixing of a circular suspension jet, and the turbulent mixing of a suspension with a clean fluid. The results of this theoretical study are valid only for extremely dilute suspensions and in only those cases where the slip between the phases is small. More significantly, this analysis neglects the effect of slip-shear forces. The latter, as we shall show, play a key role in particle migration and primarily determine the particle distribution within the mixing layer. Moreover, Soo neglects the conservation of particulate phase momentum in the normal direction.

We also, of course, have to place some limitations on the scope of this problem. Thus, we restrict ourselves to those suspensions in which the solid particles are spherical and all of the same size. Moreover, we assume that suspension is sufficiently dilute so that flow field about any particle does not interact with the flow field about any other particle. If the radius of the particles is of order 0.10 to 10.0 microns, this being the range of interest to us, the above restriction still allows significant total particulate mass content per unit volume of mixture, ρ_p . In particular we are interested in those situations in which ρ/ρ_p , where ρ is intrinsic density of the fluid, is of

order unity. We do, however, assume that the fluid phase of both the suspension and the clean fluid are identical, incompressible, and in thermal equilibrium with each other and with the particulate phase throughout the mixing process. Extensions of the result obtained to situations where this is not the case is immediate and of secondary importance on particle migration which results from transverse forces acting on the particles. Migration which is due to the Brownian effects is neglected in this study, since it cannot result in particle accumulation of the type previously mentioned. Moreover, we are not interested in the detail motion of individual particles, and consequently adopt the approach previously employed by [2, 11, 17, 19] in which the particulate phase is treated as a continuum.

The general conservation equations, required in this approach, were derived by Soo [18], Hinze [5], and Marble [11]. These, subject to the restrictions placed on our problem, become:

Fluid phase:

$$\frac{\partial u_i}{\partial x_i} = 0 \tag{1}$$

$$\rho\left(\frac{\partial u_i}{\partial t} + u_j \frac{\partial u_i}{\partial x_j}\right) = -\frac{\partial P}{\partial x_i} + \mu \nabla^2 u_i + \rho f_i - X_{P\,i} \tag{2}$$

Solid Phase: (designated by the letter -p)

$$\frac{\partial \rho_p}{\partial t} + \frac{\partial}{\partial x_i}(\rho_p u_p)_i = 0 \tag{3}$$

$$\rho_p\left(\frac{\partial u_p}{\partial t} i + u_{p_j} \frac{\partial u_p}{\partial x_j} i\right) = \rho_p f_{p\,i} + X_{P\,i} \tag{4}$$

Where X_{p_i} is the interaction force (per unit volume) between the phases. The intrinsic density of solid phase by which we mean the density of the material making up the particles is denoted by ρ_s and does not explicitly enter the above equations.

II. Interaction between the phases

Critical to any investigation of the fluid dynamics of suspensions is the modelling of the interaction between the phases. In general, the total force on an individual particle within a suspension depends upon the acceleration history of the particle, the proximity of other particles and/or walls, the particle Reynolds number, Knudsen number, as well as on the local acceleration, pressure gradient, and shear gradient of fluid field. A review of the present state of knowledge concerning these effects is given by Otterman (1968) [12], Soo (1967) [18], and Torobin and Gauvin (1959) [21]. It is concluded in [12] that our present knowledge concerning these effects is such that at the very outset we must limit our analysis to those cases where the particle Reynolds number is small. In addition it is shown that the Basset resistance (which accounts for the acceleration history) is small compared to the instantaneous Stokes drag, provided that the time scales of interest are of order τ_p, the Stokesian slip relaxation time constant, and when the particle acceleration is not extreme.

Particle motion in a spatially non-uniform velocity field results in a transverse force on the particle, even when the particle is pre-

vented from rotating. Saffman (1965) [14] in a recent study obtained the net force acting on a small translating sphere which is simultaneously rotating in an unbounded, uniform, simple shear flow field, the translation velocity being parallel to the stream lines. Three independent particle Reynolds number arise in the analysis:

$$\text{slip:} \quad (Re)_p = \frac{2a(u_p - u)}{\nu} \tag{5}$$

$$\text{shear:} \quad (Re)_K = \frac{4a^2 K}{\nu} \tag{6}$$

$$\text{rotation:} \quad (Re)_\Omega = \frac{4a^2 \Omega}{\nu} \tag{7}$$

where, the particle relative velocity $(u_p - u)$ is measured at its center, K is the magnitude of the velocity gradient, and Ω is the magnitude of the angular velocity. The analysis, which is valid when

$$(Re)_p, (Re)_K, (Re)_\Omega << 1 \quad \text{and} \quad (Re)_K, (Re)_\Omega >> (Re)_p^2$$

showed that in addition to Stokes drag force

$$D = 6\pi\mu a (u_p - u) \tag{8}$$

the particle experiences a transverse force given by

$$(L)_K = 81.2\, a^2 (\rho\mu)^{1/2} K^{1/2} (u_p - u) \tag{9}$$

which is due to the combination of slip and shear, and a lift force

which is due to rotation given by:

$$(L)_{\Omega} = \pi \rho a^3 \Omega (u_p - u) \qquad (10)$$

The latter result was also obtained by Rubinow and Keller (1961) [13]. However, Saffman's study shows that unless the rotation speed is very much greater than the rate of shear, and for freely rotating particle $\Omega = 0.5 K$, the lift force due to particle rotation is less by an order of magnitude than that due to the slip-shear (Eq. 9). Moreover, as $(R_e)_p \to 0$ Brenner [1] showed that Saffman's conditions (Eq. 8) are always met and the Rubinow-Keller theory is inapplicable.

Although direct experimental verification of Saffman's analysis is up to the present not available, an analysis of the above cited migration experiments shows that the lateral force resulting from slip-shear effect plays a significant role in these phenomena. Since boundary layer flows are characterized by large velocity gradients, and because the slip-shear lift force as given by Equation 9 is proportional to the square root of the velocity gradient we would expect, and indeed find it the case, that the particle velocities in the direction normal the main flow direction are significantly affected by this force. However, up to now this effect has not been incorporated into continuum type [3, 9, 11, 16 19] analysis of suspension flows. The only exception being the recent study of Lawler and Lu [8] in which they analyzed the behavior of a dilute suspension in the entrance region of a slowly rotating pipe. Their result which follows from a linearized model shows once again the significance of lift force on the particles.

In light of the above, we assume that the interaction between the particles and the fluid is governed by Equations 8 and 9. Strictly

speaking, these equations are applicable only for the case of linear shear field. Since the velocity profile in a laminar boundary layer is smooth, and because we are considering particles of micron size, we assume that Equations 8 and 9 can be applied locally with sufficient accuracy. In terms of a force per unit volume of mixture, the interaction between the particulate and fluid phases (Equations 8 and 9) becomes

$$\vec{X}_p = \rho_p \left[\frac{\vec{u} - \vec{u}_p}{\tau_p} + 4.5 \left(\frac{\frac{\rho}{\rho_s}}{\tau_p \left| \operatorname{curl} \vec{u} \right|} \right)^{1/2} \operatorname{curl} \vec{u} \times (\vec{u} - \vec{u}_p) \right] \tag{11}$$

where

$$\tau_p = \frac{2}{9} \left(\frac{\rho_s a^2}{\mu} \right) \tag{12}$$

III. The Two-Dimensional Suspension Boundary Layer Equations

Given the non-linear form of the interaction between the phases, Eq. 11, in addition to the non-linear form of the conservation of momentum equations of both phases, Eqs. 1 through 4, it is imperative to investigate what simplification of these equations result in the case of large Reynolds number flows. With this in mind, it is shown in [12] that the standard boundary layer approximations are valid for the fluid phase, i.e.

$$\frac{\partial P}{\partial y} = 0 \quad , \quad P = P(x,t)$$

provided that ρ_p/ρ is of order 1. Moreover, it is shown that simplification of the particulate phase momentum equations does not occur, and that the y-momentum equation cannot be neglected.

The two-dimensional boundary layer equations are specialized for the case where viscous dissipations, particle volume, Brownian motion and electric or magnetic effects are negligible; and where the fluid phase is imcompressible, the particles are all of equal and unchanging size, and the interaction between the phases is specified by Equation 11. Subject to these restrictions the continuity and boundary layer momentum equations for the two phases become:

$$\frac{\partial u}{\partial x} + \frac{\partial v}{\partial y} = 0 \tag{13}$$

$$\frac{\partial u}{\partial t} + u\frac{\partial u}{\partial x} + v\frac{\partial u}{\partial y} = -\frac{1}{\rho}\frac{dP}{dx} + \nu\frac{\partial^2 u}{\partial y^2} + \frac{\beta(u-u)}{\rho\,\tau_p} \tag{14}$$

$$\frac{\partial \rho_p}{\partial t} + \frac{\partial}{\partial x}(\rho_p u_p) + \frac{\partial}{\partial y}(\rho_p v_p) = 0 \tag{15}$$

$$\frac{\partial u_p}{\partial t} + u_p \frac{\partial u_p}{\partial x} + v_p \frac{\partial u_p}{\partial y} = \frac{(u - u_p)}{\tau_p} \tag{16}$$

$$\frac{\partial v_p}{\partial t} + u_p \frac{\partial v_p}{\partial x} + v_p \frac{\partial v_p}{\partial y} = \frac{(v - v_p)}{\tau_p} + \frac{4.5\left(\frac{\rho}{\rho_\infty}\right)^{1/2} \left|\frac{\partial u}{\partial y}\right|^{1/2} (u - u_p)}{\tau_p^{1/2}} \tag{17}$$

We now introduce the following dimensionless quantities:

$$\phi = t/\tau_p \quad , \quad \overset{*}{x} = \frac{x}{\lambda} \quad , \quad \overset{*}{y} = \frac{y}{(\tau_p \nu)^{1/2}}$$

$$\overset{*}{u} = \frac{u}{\bar{u}} \quad , \quad \overset{*}{v} = v\left(\frac{\tau_p}{\nu}\right)^{1/2} \quad , \quad \overset{*}{P} = \frac{P}{\rho \bar{u}^2} \tag{18}$$

$$\overset{*}{u}_p = \frac{u_p}{\bar{u}} \quad , \quad \overset{*}{v}_p = v_p\left(\frac{\tau_p}{\nu}\right)^{1/2} \quad , \quad \overset{*}{\rho}_p = \frac{\rho_p}{\rho_{p\infty}}$$

$$\Lambda = \left(\frac{\rho}{\rho_p}\right)_\infty = \text{constant}, \quad \Gamma = 4.5\left(\frac{\rho}{\rho_\infty}\right)^{1/2}\left(\frac{\bar{u}\lambda}{\nu}\right)^{3/4} = \text{constant}$$

Where,

$$\lambda = \tau_p \bar{u} \tag{19}$$

is termed the slip relaxation length. Physically it represents the distance required for a particle to travel in order to reduce its slip velocity by e^{-1}. Hence, as was first pointed out by Marble [11], if $x^* << 1$ the particles have not had time to adjust to the gas flow and consequently take on large velocity slips. On the other hand, if $x^* >> 1$ the particles have moved many times the required distance, and exhibit small velocity slips. For the case where the particles have a different temperature from the surrounding fluid, analagous thermal equilibration length can be developed [16].

Substitution of Equation 18 into Equations 13 through 17 yields:

$$\frac{\partial u^*}{\partial x^*} + \frac{\partial v^*}{\partial y^*} = 0 \tag{20}$$

$$\frac{\partial u^*}{\partial \phi} + u^* \frac{\partial u^*}{\partial x^*} + v^* \frac{\partial u^*}{\partial y^*} = -\frac{dp^*}{dx^*} + \frac{\partial^2 u^*}{\partial y^{*2}} + \Lambda \rho_p^* (u_p^* - u^*) \tag{21}$$

$$\frac{\partial \rho_p^*}{\partial \phi} + \frac{\partial}{\partial x^*}(\rho_p^* u_p^*) + \frac{\partial}{\partial y^*}(\rho_p^* v_p^*) = 0 \tag{22}$$

$$\frac{\partial u_p^*}{\partial \phi} + u_p^* \frac{\partial u_p^*}{\partial x^*} + v_p^* \frac{\partial u_p^*}{\partial y^*} = (u^* - u_p^*) \tag{23}$$

$$\frac{\partial v_p^*}{\partial \phi} + u_p^* \frac{\partial v_p^*}{\partial x^*} + v_p^* \frac{\partial v_p^*}{\partial y^*} = (v^* - v_p^*) + \Gamma (u^* - u_p^*) \Big/ \left| \frac{\partial u^*}{\partial y^*} \right|^{1/2} \tag{24}$$

Thus, we have successfully combined all the physical parameters governing the motion of a viscous suspension into two dimensionless constants, Λ and Γ. Equations 20 through 24 represent a "universal" set of equations which describe the basic fluid mechanics of suspension boundary layer flows. These will now be solved for the case of laminar mixing of a suspension with a clean fluid.

IV. Analysis

Consider two uniform streams which move parallel to each other with velocities u_1 and u_2 respectively, say, in the horizontal direction. Let the stream moving with velocity u_2, $u_2 > u_1$ have particles suspended in it. At $x = 0$, the suspension and the clean fluid begin to mix. Our purpose is to compute the steady-state growth of the mixing region, the slip between the phases, and the particle concentration within the mixing region.

The governing equations for this problem are Equations 20 through 24 with the time dependent terms deleted. In addition, we assume that mixing occurs at constant pressure, i.e.,

$$\frac{dP}{dx} = 0$$

For the present problem we define the characteristic velocity by:

$$\bar{u} = \frac{u_1 + u_2}{2} \tag{25}$$

and let

$$\Lambda = \frac{u_1 - u_2}{u_1 + u_2} \tag{26}$$

represent the average velocity difference of the two streams.

The boundary conditions are:

$$\begin{aligned} \overset{*}{u}(0, \overset{*}{y}) &= \overset{*}{u}_p(0, \overset{*}{y}) = 1 + \Lambda \\ \overset{*}{u}(\overset{*}{x}, \infty) &= \overset{*}{u}_p(\overset{*}{x}, \infty) = 1 + \Lambda \\ \overset{*}{u}(\overset{*}{x}, -\infty) &= 1 - \Lambda \\ \overset{*}{\rho}_p(\overset{*}{x}, \infty) &= 1 \end{aligned} \tag{27}$$

Unfortunately, Equations 20 through 24 with their accompanying boundary conditons are not amenable to an exact solution for the entire range of $\overset{*}{x}$. We therefore obtain a solution applicable in the initial portion of the mixing layer, and one valid for the far out mixing region. Both solutions are obtained in terms of the transform variables

$$\xi = \overset{*}{x}$$

$$\eta = \frac{\overset{*}{y}}{\sqrt{\overset{*}{x}}}$$

Where the initial mixing region solution is a coordinate perturbation solution in terms of ξ^n, n being positive, and the far out mixing region solution is likewise a coordinate perturbation solution where n is negative. It is readily observed that for the initial mixing region solution the boundary conditions, $\overset{*}{u}(0,\overset{*}{y}) = 1+\Lambda$, and $\overset{*}{u}(\overset{*}{x},\infty) = 1+\Lambda$ collapse into a single boundary condition at $\eta \to \infty$. The question that now arises is what sort of initial ($\overset{*}{x}=0$) boundary condition does the far out mixing region satisfy. Clearly, for it to be a valid description of our problem in the far downstream region, and not some arbitrary large ξ (small slip) solution, it also must satisfy the boundary condition $\overset{*}{u}(0,y) = 1+\Lambda$. That this indeed is the case, can be noted from the fact that $\xi^{-1} = \frac{\lambda}{\overset{*}{x}}$ expansion in the limit as $\overset{*}{x} \to \infty$ is mathematically equivalent to one in which $\lambda \to 0$. Physically, the latter represents a suspension flow in which the particles are permanantly frozen to the surrounding fluid. The flow field of such a mixture, like that of a pure fluid, is similar in the variable η (which is independent of λ) and, moreover, satisfies the boundary conditions at $\overset{*}{x} = 0$. Consequently, the zeroth order term of ξ^{-1} expansion also satisfies the initial condition at $\overset{*}{x} = 0$. Finally, it should be noted that the analysis which

follows is parallel to the one developed by Singleton [17] for flow over a semi-infinite flat plate in which slip-shear forces were not incorporated.

The Initial Mixing Region

At the start of the mixing region, to zeroth order, the two phases flow independently of each other. This suggests a solution in terms of a separate stream function for each phase. We define $\overset{*}{\psi}$ and $\overset{*}{\psi}_p$, the dimensionless fluid and particulate phase stream functions, by:

$$\overset{*}{u} = \frac{\partial \overset{*}{\psi}}{\partial \overset{*}{y}} \quad , \quad \overset{*}{v} = -\frac{\partial \overset{*}{\psi}}{\partial \overset{*}{x}} \tag{28}$$

$$\overset{*}{\rho}_p \overset{*}{u}_p = \frac{\partial \overset{*}{\psi}_p}{\partial \overset{*}{y}} \quad , \quad \overset{*}{\rho}_p \overset{*}{v}_p = -\frac{\partial \overset{*}{\psi}_p}{\partial \overset{*}{x}} \tag{29}$$

Note that the defined stream functions satisfy identically the fluid and particulate phase continuity relations. Substituting Equations 33 and 34 into Equations 21, 23 and 24 we obtain:

$$\frac{\partial \overset{*}{\psi}}{\partial \overset{*}{y}} \frac{\partial^2 \overset{*}{\psi}}{\partial \overset{*}{x} \partial \overset{*}{y}} - \frac{\partial \overset{*}{\psi}}{\partial \overset{*}{x}} \frac{\partial^2 \overset{*}{\psi}}{\partial \overset{*}{y}^2} = \frac{\partial^3 \overset{*}{\psi}}{\partial \overset{*}{y}^3} + \lambda \left(\frac{\partial \overset{*}{\psi}_p}{\partial \overset{*}{y}} - \overset{*}{\rho}_p \frac{\partial \overset{*}{\psi}}{\partial \overset{*}{y}} \right) \tag{30}$$

$$\frac{\partial \overset{*}{\psi}_p}{\partial \overset{*}{y}} \left(\overset{*}{\rho}_p \frac{\partial^2 \overset{*}{\psi}_p}{\partial \overset{*}{x} \partial \overset{*}{y}} - \frac{\partial \overset{*}{\rho}_p}{\partial \overset{*}{x}} \frac{\partial \overset{*}{\psi}_p}{\partial \overset{*}{y}} \right) - \frac{\partial \overset{*}{\psi}_p}{\partial \overset{*}{x}} \left(\overset{*}{\rho}_p \frac{\partial^2 \overset{*}{\psi}_p}{\partial \overset{*}{y}^2} - \frac{\partial \overset{*}{\rho}_p}{\partial \overset{*}{y}} \frac{\partial \overset{*}{\psi}_p}{\partial \overset{*}{y}} \right)$$

$$= \left(\overset{*}{\rho}_p^3 \frac{\partial \overset{*}{\psi}}{\partial \overset{*}{y}} - \overset{*}{\rho}_p^2 \frac{\partial \overset{*}{\psi}_p}{\partial \overset{*}{y}} \right) \tag{31}$$

$$\frac{\partial \overset{*}{\psi}_p}{\partial \overset{*}{y}}\left(\overset{*}{\rho}_p \frac{\partial^2 \overset{*}{\psi}_p}{\partial \overset{*}{x}^2} - \frac{\partial \overset{*}{\rho}_p}{\partial \overset{*}{x}} \frac{\partial \overset{*}{\psi}_p}{\partial \overset{*}{x}}\right) - \frac{\partial \overset{*}{\psi}_p}{\partial \overset{*}{x}}\left(\overset{*}{\rho}_p \frac{\partial^2 \overset{*}{\psi}_p}{\partial \overset{*}{y}\partial \overset{*}{x}} - \frac{\partial \overset{*}{\rho}_p}{\partial \overset{*}{y}} \frac{\partial \overset{*}{\psi}_p}{\partial \overset{*}{x}}\right)$$

$$= \left(\overset{*}{\rho}_p^3 \frac{\partial \overset{*}{\psi}}{\partial \overset{*}{x}} - \overset{*}{\rho}_p^2 \frac{\partial \overset{*}{\psi}_p}{\partial \overset{*}{x}}\right) + J\left(\overset{*}{\rho}_p^2 \frac{\partial \overset{*}{\psi}_p}{\partial \overset{*}{y}} - \overset{*}{\rho}_p^3 \frac{\partial \overset{*}{\psi}}{\partial \overset{*}{y}}\right)\left|\frac{\partial^2 \overset{*}{\psi}}{\partial \overset{*}{y}^2}\right|^{1/2} \tag{32}$$

Introducing the transform defined by:

$$\xi = \overset{*}{x} \tag{33}$$

$$\eta = \frac{\overset{*}{y}}{\sqrt{\overset{*}{x}}} \tag{34}$$

into Equations 30 through 31 we obtain:

$$\frac{\partial \overset{*}{\psi}}{\partial \eta}\left(\frac{\partial^2 \overset{*}{\psi}}{\partial \xi \partial \eta} - \frac{1}{2\xi}\frac{\partial \overset{*}{\psi}}{\partial \eta}\right) - \frac{\partial \overset{*}{\psi}}{\partial \xi}\frac{\partial^2 \overset{*}{\psi}}{\partial \eta^2} = \frac{1}{\xi^{1/2}}\frac{\partial^3 \overset{*}{\psi}}{\partial \eta^3} + \xi^{1/2}\left(\frac{\partial \overset{*}{\psi}_p}{\partial \eta} - \overset{*}{\rho}_p \frac{\partial \overset{*}{\psi}}{\partial \eta}\right) \tag{35}$$

$$\overset{*}{\rho}_p \frac{\partial \overset{*}{\psi}_p}{\partial \eta}\left(\frac{\partial^2 \overset{*}{\psi}_p}{\partial \xi \partial \eta} - \frac{1}{2\xi}\frac{\partial \overset{*}{\psi}_p}{\partial \eta}\right) - \left(\frac{\partial \overset{*}{\psi}_p}{\partial \eta}\right)^2 \frac{\partial \overset{*}{\rho}_p}{\partial \xi}$$

$$+ \frac{\partial \overset{*}{\psi}_p}{\partial \xi}\left(\frac{\partial \overset{*}{\rho}_p}{\partial \eta}\frac{\partial \overset{*}{\psi}_p}{\partial \eta} - \overset{*}{\rho}_p \frac{\partial^2 \overset{*}{\psi}_p}{\partial \eta^2}\right)$$

$$= \xi\left(\overset{*}{\rho}_p^3 \frac{\partial \overset{*}{\psi}}{\partial \eta} - \overset{*}{\rho}_p^2 \frac{\partial \overset{*}{\psi}_p}{\partial \eta}\right) \tag{36}$$

$$\left(\frac{\partial^2 \eta_R}{\partial \hat{\psi}_R^2}\right)\left(\frac{\eta_R}{\hat{\psi}_R^d} - \frac{\eta_R}{\hat{\psi}_R^*}\right)\hat{\delta}_p^{d\,2}\hat{\delta}_p^{*\,2}\Bigg] \tag{37}$$

$$= \xi\left[\hat{\delta}_p^{*\,2}\left(\frac{\xi_R}{\hat{\psi}_R^*} - \frac{\xi_R}{\eta}\frac{\eta_R}{\hat{\psi}_R^*}\hat{\delta}_p^{d} - \frac{\xi_R}{\eta}\frac{\eta_R}{\hat{\psi}_R^*}\hat{\delta}_p^{d}\right)\right]$$

$$+\left[\left(\frac{\eta_R}{\hat{\psi}_R^d}\frac{\xi_R}{\eta} - \frac{2\eta_R}{\hat{\psi}_R^{*2}}\frac{\xi_R}{\eta} - \frac{\xi_R\eta_R}{\hat{\psi}_R^{*2}\eta}\right)\frac{\xi_R}{\hat{\psi}_R^*}\hat{\delta}_p^{d}\hat{\delta}_p^{*}\right] + \xi^{1/2}\left[\left(\frac{\eta_R}{\hat{\psi}_R^*}\frac{\xi^2}{\eta} - \frac{\xi_R}{\hat{\psi}_R^*}\right)\right.$$

$$\left.+\left[\left(\frac{\eta_R}{\hat{\psi}_R^d}\frac{\xi_R\eta_R}{\eta} - \frac{2\eta_R}{\hat{\psi}_R^{*2}}\frac{\xi^2}{\eta} - \frac{\xi_R\eta_R}{\hat{\psi}_R^{*2}\eta}\right)\frac{\xi_R}{\hat{\psi}_R^*}\hat{\delta}_p^{d}\hat{\delta}_p^{*}\right] + \xi^{1/2}\left[\left(\frac{\eta_R}{\hat{\psi}_R^*}\frac{\xi^2}{\eta} - \frac{\xi_R}{\hat{\psi}_R^*}\right)\right.\right.$$

$$\left.\left.+\left[\left(\frac{\eta_R}{\hat{\psi}_R^d}\frac{\xi^2}{\eta} - \frac{\xi_R}{\hat{\psi}_R^*}\right)\frac{\xi_R}{\hat{\psi}_R^d}\hat{\delta}_p^{d}\hat{\delta}_p^{*}\right] + \xi^{1/2}\left[\frac{\xi_R}{\hat{\psi}_R^*}\frac{\eta_R}{\hat{\psi}_R^d} - \left(\frac{\eta_R}{\hat{\psi}_R^d}\frac{\xi^2}{\eta} - \frac{\xi_R}{\hat{\psi}_R^*}\right)\frac{\xi_R}{\hat{\psi}_R^d}\frac{\eta_R}{\hat{\psi}_R^*}\right]\xi^{1/2}\right.\right.$$

The initial mixing is characterized by $\xi \ll 1$. Consequently, we assume the following expansions for $\overset{*}{\psi}$, $\overset{*}{\psi}_p$, and $\overset{*}{\rho}_p$.

$$\overset{*}{\psi} = \xi^{1/2}\left(f_0(\eta) + \xi f_1(\eta) + \xi^{5/4} f_2(\eta) + \cdots\right) \tag{38}$$

$$\overset{*}{\psi}_p = \xi^{1/2}\left(h_0(\eta) + \xi h_1(\eta) + \xi^{5/4} h_2(\eta) + \cdots\right) \tag{39}$$

$$\overset{*}{\rho}_p = 1 + \xi K_1(\eta) + \xi^{5/4} K_2(\eta) + \cdots \tag{40}$$

Substituting these expansions into Equations 35 through 37 and equating coefficients of ξ^n to zero yields the following:

Equation 35 gives in the zeroth order

$$f_0''' + \tfrac{1}{2} f_0 f_0'' = 0 \tag{41}$$

while Equations 36 and 37 yield respectively

$$\tfrac{1}{2} h_0 h_0'' = 0$$

and

$$\eta h_0'' h_0 - \eta (h_0')^2 + h_0' h_0 = 0$$

Therefore,

$$h_0'(h_0 - \eta h_0') = 0$$

but since $h_0' \neq 0$, Equation 42 yields

$$h_0 = C\eta$$

where C is a proportion constant.

Moreover, since, $h_o'(\infty) = 1+\Lambda$, we obtain:

$$h_o = (1+\Lambda)\eta \tag{43}$$

Thus, to the zeroth order the two phases flow independently of each other.

The flow field of the fluid phase is governed by the Blasius equation (Eq.41) which for the present case of laminar mixing is subject to the following boundary conditions:

$$f_o'(+\infty) = 1+\Lambda \tag{44}$$

$$f_o'(-\infty) = 1-\Lambda \tag{45}$$

Note that we are given only two boundary conditions for a third order differential equation. In order to determine the solution exactly we take

$$f_o(o) = 0 \tag{46}$$

Equation 46 specifies that $\eta = 0$ is a stream line. Since, $\eta = 0$ corresponds to the line y = 0, in essence we have assumed that the interface of the two streams remains located along this line. More likely, this interface will bend and deviate from the original line of contact. Suppose we now write the two phase conservation equations in terms of curvilinear orthogonal coordinate system, whose x-axis is in the direction of the interface, and y perpendicular to it. If we now assume that the curvature of the interface is small, these equations reduce to the governing Equations 22through 26. We feel that this assumption is reasonable, and represents an appropriate approximation for a "first round"

theoretical solution to a problem for which experimental data is not available.

Goertler (4) in a paper on turbulent mixing of two fluid streams suggests the following method of solution for the Blasius equation subject to the above boundary conditions. Let

$$f_0 = 2\sum_{n=0}^{\infty} \lambda^n \mu_n(\gamma) \tag{47}$$

where, $\gamma = \eta/2 = \mu_0$

Substituting this expansion into Equation 41 gives:

$$\mu_1''' + 2\gamma\,\mu_1'' = 0 \tag{48}$$

$$\mu_2''' + 2\gamma\,\mu_2'' = -2\mu_1\mu_1'' \tag{49}$$

$$\mu_3''' + 2\gamma\,\mu_3'' = -2\left(\mu_1\mu_2'' + \mu_2\mu_1''\right) \tag{50}$$

$$\vdots \qquad \vdots \qquad \vdots$$

subject to the following boundary conditions:

$$\mu_1(0) = 0 \tag{51}$$

$$\mu_1'(\gamma) = \begin{cases} 1 & \text{for } \gamma \to \infty \\ -1 & \text{for } \gamma \to -\infty \end{cases} \tag{52}$$

$$\mu_n(\gamma) = 0 \quad \begin{cases} \text{for} \\ n \geq 2 \end{cases} \quad \gamma = \pm\infty \tag{53}$$

$$\mu_n(0) = 0 \quad \{\text{for } n \geq 2 \tag{54}$$

The solution of Equation 48 subject to Equations 51 and 52 is:

$$\mu_1(\gamma) = \int_0^{\gamma} \omega(x)\, dx \tag{55}$$

where

$$\omega(x) = \frac{2}{\sqrt{\pi}} \int_0^{x} e^{-z^2}\, dz$$

$$= erf(x) \tag{56}$$

We approximate the fluid phase velocity by the first two terms of the expansion, i.e.,

$$f_0' = (1 + \Lambda\, erf(\eta/2)) \tag{57}$$

as shown in Figure 1.
The first order modification to the fluid phase stream function, $f_1(\eta)$ is obtained from Equation 35 which yields:

$$f_1''' + \tfrac{1}{2} f_0 f_1'' - f_0' f_1' + \tfrac{3}{2} f_0'' f_1 = \Lambda\left(f_0' - (1+\Lambda)\right) \tag{58}$$

We now define

$$\phi_1 = \frac{f_1(\eta)}{\Lambda\Lambda} \tag{59}$$

Equation 58 can now be written as:

$$\phi_1''' + \tfrac{1}{2} f_0 \phi_1'' - f_0' \phi_1' + \tfrac{3}{2} f_0'' \phi_1 = \left(erf(\eta/2) - 1\right) \tag{60}$$

The boundary conditions are:

$$\phi_1'(\infty) = 0$$
$$\phi_1''(0) = 0 \qquad (61)$$
$$\phi_1(0) = 0$$

Equation 60 subject to the above boundary conditions was solved numerically and the results are given in Figure 2. Note that since the particulate phase leads the fluid phase, the first order modification on the fluid velocity, $f_1'(\eta)$, is positive. The first order functions $h_1(\eta)$ and $K_1(\eta)$ as obtained from Equations 36 and 37 are:

$$\eta^2 H_1'' - 3\eta H_1' + 3H_1 = 2(f_0 - \eta f_0') \qquad (62)$$

$$(1+\Lambda)^2(\eta K_1' - 2K_1) = \eta H_1'' - 2H_1 + 2\left[f_0' - (1+\Lambda)\right] \qquad (63)$$

where,

$$H_1(\eta) = (1+\Lambda)h_1(\eta) \qquad (64)$$

The complimentary solution of Equation 62 is:

$$C_1\eta + C_2\eta^3$$

By the method of variation of parameters, i.e.,

$$H_1(\eta) = \eta^3 A(\eta) + \eta B(\eta)$$

we obtain for the above particular solution

$$A(\eta) = -\frac{f_0(\eta)}{\eta^3} + 2\int_\eta^\infty \frac{f_0(x)}{x^4}\,dx \qquad (65)$$

$$B(\eta) = \frac{f_0(\eta)}{\eta}. \qquad (66)$$

Therefore, the complete solution is

$$H_1(\eta) = 2\eta^3 \int_\eta^\infty \frac{f_o(x)}{x^4}\, dx + C_1\eta + C_2\eta^3 \tag{67}$$

and

$$H_1'(\eta) = 6\eta^2 \int_\eta^\infty \frac{f_o(x)}{x^4}\, dx - 2\frac{f_o(\eta)}{\eta} + C_1 + 3C_2\eta^2 \tag{68}$$

Note that

$$\lim_{\eta\to\infty} \frac{f_o(\eta)}{\eta} = 1 - \Lambda \tag{69}$$

and

$$\lim_{\eta\to-\infty} \frac{f_o(\eta)}{\eta} = 1 - \Lambda \tag{70}$$

Since, $H_1'(\infty) = 0$, we obtain $C_2 = 0$ and $C_1 = -(1+\Lambda)$, consequently,

$$H_1'(\eta) = 6\eta^2 \int_\eta^\infty \frac{f_o(x)}{x^4}\, dx - 2\frac{f_o(\eta)}{\eta} - (1+\Lambda) \tag{71}$$

The above expression seems quite reasonable, since in the regime of large particle slip, the particles do not have sufficient time to adjust to local flow conditions, and thus the velocity would also depend on their initial conditions, $(1+\Lambda)$, and on integrated effect of their motion through the flow field. This is in sharp contrast to what will occur in the regime of small slip, where we shall find the particulate phase velocity only a function of the local flow conditions. Finally,

we can show that

$$\lim_{\eta \to 0} h_1'(\eta) = -\lambda/(1+\lambda) \tag{72}$$

A graphical representation of $h_1'(\eta)$ as obtained by numerical integration is given in Figure 3. The first order particulate phase velocity in the horizontal direction, $h_1'(\eta)$, is negative becuase the decelerating fluid phase exerts a drag force on the particulate phase. In addition, the latter experiences a drag force in the y-direction. The resulting velocity is given by:

$$\overset{*}{U}_p^{(1)} = \varepsilon^{1/2}\left(\eta/2\, h_1' - 3/2\, h_1\right) \tag{73}$$

A plot of $\overset{*}{U}_p^{(1)}$ is given in Figure 4. Observe that the effect of this velocity is to transport the particulate phase away from the clean fluid region.

The first order modification to the free stream particulate phase density is given by Equation 6 3 . The latter, after substitution for $h_1'(\eta)$ and $h_1''(\eta)$ becomes:

$$\eta K_1' - 2K_1 = 0 \tag{74}$$

which after integration yields:

$$K_1 = C_1 \eta^2 \tag{75}$$

Since $K_1(\infty) = 0$ it must be that $C_1 = 0$, consequently,

$$K_1(\eta) = 0 \tag{76}$$

i.e., at the start of the mixing region where $\xi << 1$, the drag effects do not result in a change of the particulate phase density. This implies that in this region, the increase in the particulate phase density resulting from the slowing down of the phase in the x-direction, is identically counterbalanced by the removal of the particles from the boundary layer in the positive y-direction. The higher order terms of Equations 37 and 36 are respectively:

$$K_2' - \frac{5}{2\eta} K_2 = h_2'' - \frac{5}{2\eta} h_2' \tag{77}$$

$$\eta^2 h_2'' - 4\eta h_2' + \frac{21}{4} h_2 = \frac{\Gamma}{1+\Lambda} (f_0'')^{1/2} (h_0' - f_0') \tag{78}$$

Equation 77 is immediately integratable and yields:

$$K_2 = h_2'(\eta) \tag{79}$$

since $K_2(\infty) = h'_2(\infty) = 0$. Defining,

$$H_2 = \frac{h_2(1+\Lambda)}{\Gamma \Lambda^{3/2}} \tag{80}$$

Equation 78 becomes:

$$\eta^2 H_2'' - 4\eta H_2' + \frac{21}{4} H_2 = F(\eta) \tag{81}$$

where

$$F(\eta) = 4(h_0' - f_0')(f_0'')^{1/2}$$

$$= \frac{4}{(\pi)^{1/4}}\left(1 - \operatorname{erf}(\eta/2)\right) e^{-1/8\,\eta^2} \qquad (82)$$

The solution to the homogenous part of Equation 81 is:

$$H_2(\eta) = \eta^{3/2} A(\eta) + \eta^{7/2} B(\eta) \qquad (83)$$

Again, using the method of variation of parameters, we obtain:

$$A(\eta) = \frac{1}{2}\int_{\eta}^{\infty} \frac{F(x)}{x^{5/2}}\,dx \qquad (84)$$

$$B(\eta) = -\frac{1}{2}\int_{\eta}^{\infty} \frac{F(x)}{x^{9/2}}\,dx \qquad (85)$$

Therefore, the complete solution is

$$H_2(\eta) = \frac{1}{2}\eta^{3/2}\int_{\eta}^{\infty} \frac{F(x)}{x^{5/2}}\,dx - \frac{1}{2}\eta^{7/2}\int_{\eta}^{\infty} \frac{F(x)}{x^{9/2}}\,dx + C_1\eta^{3/2} + C_2\eta^{7/2} \qquad (86)$$

and hence

$$H_2'(\eta) = \frac{3}{4}\eta^{1/2}\int_{\eta}^{\infty} \frac{F(x)}{x^{5/2}}\,dx - \frac{7}{4}\eta^{5/2}\int_{\eta}^{\infty} \frac{F(x)}{x^{9/2}}\,dx + \frac{3}{2}C_1\eta^{1/2} + \frac{7}{2}C_2\eta^{5/2}$$

Since $H_2'(\infty) = 0$, $C_1 = C_2 = 0$, we have

$$H_2'(\eta) = \frac{3}{4}\eta^{1/2}\int_{\eta}^{\infty} \frac{F(x)}{x^{5/2}}\,dx - \frac{7}{4}\eta^{5/2}\int_{\eta}^{\infty} \frac{F(x)}{x^{9/2}}\,dx \qquad (87)$$

the clean fluid region. The corresponding decrease in the particulate phase density of the suspension is determined by Equation 88. We can show that

$$\lim_{\eta \to 0} K_2 = \frac{8}{10} \lim_{\eta \to 0} \frac{F(\eta)}{\eta}$$

Since $F(0) = \frac{4}{(\pi)^{1/4}}$, K_2 is singular at $\eta = 0$. This result is in agreement with our notion that in the neighborhood of $\eta = 0$, the basic assumption of a particulate continuum would become invalid, due to particle depletion. For $\eta > 0$, $K_2(\eta)$ is well behaved as is illustrated in Figure 6. Finally, observe that $f_0(\eta)$, $f_1(\eta)/\Lambda s$, $h_1'(\eta)/\Lambda$, $(1+\Lambda)h_2(\eta)/\Gamma\Lambda^{3/2}$, and $K_2(\eta)$ are universal functions of η, once calculated provide the first order solution (in the context of the assumption made in the analysis) for the problem of mixing of any solid particle-fluid suspension with a clean fluid.

The Far Out Mixing Region:

In the limit as $\xi \to \infty$, the slip between the phases approaches zero and the suspension flows as a single continuous phase. Therefore, to the zeroth order, the region specified by $(\xi, \eta \geq 0)$ is characterized by the flow of a fluid stream of density $\rho(H\rho)$ and viscosity μ. On the other hand, the particulate density of the originally clean stream at distances far downstream from the initial point of contact is small, since the particulate phase which was injected into it has become diluted by the continual addition of clean fluid. Consequently in the far downstream region, the problem corresponds to the mixing of two streams of equal viscosity but of different density. We take this into account

by defining a fluid stream function, $\overset{*}{\psi}_1$, for $\eta \geq 0$, and another, $\overset{*}{\psi}_2$, for $\eta \leq 0$. Where,

$$\eta \geq 0 \quad , \overset{*}{u} = \frac{\partial \overset{*}{\psi}_1}{\partial \overset{*}{y}} \quad , \overset{*}{v} = -\frac{\partial \overset{*}{\psi}_1}{\partial \overset{*}{x}} \tag{92}$$

$$\eta \leq 0 \quad , \quad \overset{*}{u} = \frac{\partial \overset{*}{\psi}_2}{\partial \overset{*}{y}} \quad , \quad \overset{*}{v} = -\frac{\partial \overset{*}{\psi}_2}{\partial \overset{*}{x}} \tag{93}$$

which identically satisfy the fluid continuity, Equation 20.

A continuum discription of the particulate phase in the far downstream region and for $\eta < 0$ is not valid because of the vanishingly small particulate density. For $\eta \geq 0$ we describe the velocity of the particulate phase in terms of slip velocities,

$$\begin{aligned} \overset{*}{u}_s &= \overset{*}{u}_p - \overset{*}{u} \\ \overset{*}{v}_s &= \overset{*}{v}_p - \overset{*}{v} \end{aligned} \tag{94}$$

since we expect that the latter are of order $1/S$. The X- and Y-momentum equations of the solid phase (Eq.'s 23 and 24) in terms of the slip velocities become:

$$\overset{*}{u}_s \left[\frac{\partial \overset{*}{u}_s}{\partial \overset{*}{x}} + \frac{\partial \overset{*}{u}}{\partial \overset{*}{x}} \right] + \overset{*}{u} \left[\frac{\partial \overset{*}{u}_s}{\partial \overset{*}{x}} + \frac{\partial \overset{*}{u}}{\partial \overset{*}{x}} \right]$$

$$+ \overset{*}{v}_s \left[\frac{\partial \overset{*}{u}_s}{\partial \overset{*}{y}} + \frac{\partial \overset{*}{u}}{\partial \overset{*}{y}} \right] + \overset{*}{v} \left[\frac{\partial \overset{*}{u}_s}{\partial \overset{*}{y}} + \frac{\partial \overset{*}{u}}{\partial \overset{*}{y}} \right] = -\overset{*}{u}_s \tag{95}$$

$$u_s^*\left(\frac{\partial u^*}{\partial x^*}+\frac{\partial u_s^*}{\partial x^*}\right)+u^*\left(\frac{\partial u^*}{\partial x^*}+\frac{\partial u_s^*}{\partial x^*}\right)+v_s^*\left(\frac{\partial u_s^*}{\partial y^*}+\frac{\partial u^*}{\partial y^*}\right)$$

$$+v^*\left(\frac{\partial u^*}{\partial y^*}+\frac{\partial u_s^*}{\partial y^*}\right)=-f_s^*-\tau u_s^*\left|\frac{\partial u^*}{\partial y^*}\right|^{1/2} \tag{96}$$

and the particulate phase continuity equation becomes:

$$\rho_p^*\left[\frac{\partial u_s^*}{\partial x^*}+\frac{\partial v_s^*}{\partial y^*}\right]+\frac{\partial p_p^*}{\partial x^*}(u_s^*+u^*)+\frac{\partial p_p^*}{\partial y^*}(v_s^*+v^*)=0 \tag{97}$$

The respective fluid phase momentum equations for the regions $(\xi, \eta \geq 0)$ and $(\xi, \eta \leq 0)$ are:

$$\frac{\partial \psi_1^*}{\partial y^*}\frac{\partial^2 \psi_1^*}{\partial x^* \partial y^*}-\frac{\partial \psi_1^*}{\partial x^*}\frac{\partial^2 \psi_1^*}{\partial y^{*2}}=\frac{\partial^3 \psi_1^*}{\partial y^{*3}}+\Lambda \rho_p^* u_s^* \tag{98}$$

$$\frac{\partial \psi_2^*}{\partial y^*}\frac{\partial^2 \psi_2^*}{\partial x^* \partial y^*}-\frac{\partial \psi_2^*}{\partial x^*}\frac{\partial^2 \psi_2^*}{\partial y^{*2}}=\frac{\partial^3 \psi_2^*}{\partial y^{*3}} \tag{99}$$

Once again we define the transformation,

$$\eta=\frac{y^*}{\sqrt{x^*}} \tag{100}$$

$$\xi=x^* \tag{101}$$

Equations 95 through 99 in terms of the transform variables become:

$$\left(u_s^*+\frac{1}{\xi^{1/2}}\frac{\partial \psi_1^*}{\partial \eta}\right)\left(\frac{\partial u_s^*}{\partial \xi}+\frac{1}{\xi^{1/2}}\frac{\partial^2 \psi_1^*}{\partial \xi \partial \eta}\right)-\frac{\eta}{2\xi}\left(u_s^*+\frac{1}{\xi^{1/2}}\frac{\partial \psi_1^*}{\partial \eta}\right)$$

$$+\left(\frac{\partial u_s^*}{\partial \eta}+\frac{1}{\xi^{1/2}}\frac{\partial^2 \psi_1^*}{\partial \eta^2}\right)+\frac{v_s^*}{\xi^{1/2}}\left(\frac{\partial u_s^*}{\partial \eta}+\frac{1}{\xi^{1/2}}\frac{\partial^2 \psi_1^*}{\partial \eta^2}\right)$$

$$+\frac{1}{\xi^{1/2}}\left(\frac{\partial \psi_1^*}{\partial \xi}+\frac{\eta}{2\xi}\frac{\partial \psi_1^*}{\partial \eta}\right)\left(\frac{\partial u_s^*}{\partial \eta}+\frac{1}{\xi^{1/2}}\frac{\partial^2 \psi_1^*}{\partial \eta^2}\right)=-u_s^* \tag{102}$$

$$\left(\overset{*}{u}_1+\frac{1}{\xi^{1/2}}\frac{\partial\overset{*}{\psi}_1}{\partial\eta}\right)\left(-\frac{\partial^2\overset{*}{\psi}_1}{\partial\xi^2}+\frac{\kappa}{\xi}\frac{\partial^2\overset{*}{\psi}_1}{\partial\eta\partial\xi}-\frac{3}{4}\frac{\kappa}{\xi^2}\frac{\partial\overset{*}{\psi}_1}{\partial\eta}-\frac{\eta^2}{4\xi^2}\frac{\partial^2\overset{*}{\psi}_1}{\partial\eta^2}\right.$$

$$\left.+\frac{\partial\overset{*}{v}_1}{\partial\xi}-\frac{\kappa}{2\xi}\frac{\partial\overset{*}{v}_1}{\partial\eta}\right)+\frac{v_1}{\xi^{1/2}}\left(\frac{\partial\overset{*}{v}_1}{\partial\eta}-\frac{\partial\overset{*}{\psi}_1}{\partial\eta\partial\xi}+\frac{\kappa}{2\xi}\frac{\partial^2\overset{*}{\psi}_1}{\partial\eta^2}\right)$$

$$+\frac{1}{\xi^{1/2}}\left(-\frac{\partial\overset{*}{\psi}_1}{\partial\xi}+\frac{\kappa}{2\xi}\frac{\partial\overset{*}{\psi}_1}{\partial\eta}\right)\left(-\frac{\partial\overset{*}{\psi}_1}{\partial\xi\partial\eta}+\frac{1}{2\xi}\frac{\partial\overset{*}{\psi}_1}{\partial\eta}+\frac{\kappa}{2\xi}\frac{\partial^2\overset{*}{\psi}_1}{\partial\eta^2}+\frac{\partial\overset{*}{v}_1}{\partial\eta}\right)$$

$$=\overset{*}{v}_1+\Gamma\xi^{-1/4}\overset{*}{u}_1\left|\frac{\partial^2\overset{*}{\psi}_1}{\partial\eta^2}\right|^{1/2} \tag{103}$$

$$\overset{*}{\rho}_p\left[\frac{\partial\overset{*}{u}_p}{\partial\xi}-\frac{\kappa}{2\xi}\frac{\partial\overset{*}{u}_p}{\partial\eta}+\frac{1}{\xi^{1/2}}\frac{\partial\overset{*}{v}_p}{\partial\eta}\right]+(\overset{*}{u}_1+\overset{*}{u})\left[\frac{\partial\overset{*}{\rho}_p}{\partial\xi}-\frac{\kappa}{2\xi}\frac{\partial\overset{*}{\rho}_p}{\partial\eta}\right]$$

$$+\frac{1}{\xi^{1/2}}\frac{\partial\overset{*}{\rho}_p}{\partial\eta}(\overset{*}{v}_1+\overset{*}{v})=0 \tag{104}$$

$$\frac{\partial\overset{*}{\psi}_1}{\partial\eta}\left(\frac{\partial^2\overset{*}{\psi}_1}{\partial\eta\partial\xi}-\frac{1}{2\xi}\frac{\partial\overset{*}{\psi}_1}{\partial\eta}\right)-\frac{\partial\overset{*}{\psi}_1}{\partial\xi}\frac{\partial^2\overset{*}{\psi}_1}{\partial\eta^2}=\frac{1}{\xi^{1/2}}\frac{\partial^3\overset{*}{\psi}_1}{\partial\eta^3}+\Lambda S\overset{*}{\rho}_p\overset{*}{u}_1 \tag{105}$$

$$\frac{\partial \overset{*}{\psi}_2}{\partial \eta}\left(\frac{\partial^2 \overset{*}{\psi}_2}{\partial \eta \partial \xi} - \frac{1}{2\xi}\frac{\partial \overset{*}{\psi}_2}{\partial \eta}\right) - \frac{\partial \overset{*}{\psi}_2}{\partial \xi}\frac{\partial^2 \overset{*}{\psi}_2}{\partial \eta^2} = \frac{1}{\xi^{1/2}}\frac{\partial^3 \overset{*}{\psi}_2}{\partial \eta^3} \qquad (106)$$

We now assume the following expansions for the dependent variables $\overset{*}{\psi}_1$, $\overset{*}{\psi}_2$, $\overset{*}{u}_s$, $\overset{*}{v}_s$, and $\overset{*}{\rho}_p$.

$$\overset{*}{\psi}_1 = \left(\frac{\xi}{s+1}\right)^{1/2}\left(f_0(\eta) + \xi^{-3/4} f_3(\eta) + \xi^{-1} f_4(\eta) + \cdots\right) \qquad (107)$$

$$\overset{*}{\psi}_2 = \xi^{1/2}\left(g_0(\eta) + \xi^{-3/4} g_3(\eta) + \xi^{-1} g_4(\eta) + \cdots\right) \qquad (108)$$

$$\overset{*}{u}_s = \xi^{-1} h_4(\eta) + \xi^{-5/4} h_5(\eta) + \xi^{-6/4} h_6(\eta) + \cdots \qquad (109)$$

$$\overset{*}{v}_s = \xi^{-5/4} q_5(\eta) + \xi^{-6/4} q_6(\eta) + \xi^{-7/4} q_7(\eta) + \cdots \qquad (110)$$

$$\overset{*}{\rho}_p = 1 + \xi^{-3/4} K_3(\eta) + \xi^{-1} K_4(\eta) + \xi^{-5/4} K_5(\eta) + \cdots \qquad (111)$$

Where the factor $(s + 1)^{1/2}$ in Equation 107 accounts for the fact that in the zeroth order the particles affect the fluid only through their mass. Substituting the above expansions into Equation 105 and equating the sum of coefficients of term of equal power in ξ to zero yields:

$$-\frac{1}{2} f_0 f_0'' = (s+1)^{1/2} f_0''' + s(s+1) h_4(\eta) \qquad (112)$$

$$-\frac{3}{4} f_0' f_3' - \frac{1}{2} f_0 f_3'' + \frac{1}{4} f_0'' f_3 = (s+1)^{1/2} f_3''' + s(s+1) K_3 h_4 \qquad (113)$$

plus higher order terms. While the zeroth order part of Equations 102 and 103 are respectively:

$$h_4 = \frac{1}{2(s+1)} f_o'' f_o \tag{114}$$

$$g_s = -\Gamma h_4(\eta)(f_o'')^{1/2} \tag{115}$$

Combining Equations 112 and 114 we obtain:

$$(s+1)^{1/2} f_o''' + \frac{1}{2}(s+1) f_o'' f_o = 0 \tag{116}$$

Let,

$$\overset{*}{\eta} = \eta (s+1)^{1/2} \tag{117}$$

Therefore,

$$\frac{d^3 f_o}{d\overset{*}{\eta}^3} + \frac{1}{2} f_o \frac{d^2 f_o}{d\overset{*}{\eta}^2} = 0 \tag{118}$$

Let,

$$f_o(\overset{*}{\eta}) = F_o(\overset{*}{\eta}) \tag{119}$$

Therefore,

$$F_o''' + \frac{1}{2} F_o F_o'' = 0 \tag{120}$$

Thus, as expected, the zeroth order approximation of the suspension flow corresponds to a Blasius distribution but in terms of a vertical scale modified to account for the mixture density ratio. On the other hand, the zeroth order approximation of the flow in the lower stream is given by:

$$g_0'''(\eta) + \frac{1}{2} g_0 g_0''(\eta) = 0 \qquad (121)$$

Where the connected boundary conditions for Equation 120 and 121 are given by:

$$\begin{aligned} F_0'(\infty) &= 1+\Lambda \\ g_0'(-\infty) &= 1-\Lambda \\ F_0(0) &= g_0(0) = 0 \\ (\Lambda+1)^{1/2} F_0''(0) &= g_0'''(0) \end{aligned} \qquad (122)$$

The last listed boundary condition insures continuity of tangential stress, and consequently of pressure across the interface. It should be noted that throughout this study we have neglected the shear contribution of the particle layer located at the interface, since the latter results in higher order modification of the fluid phase velocity fields. For the far downstream region, this approximation is further justified because the zeroth order slip velocity, $h_4(0) = 0$.

The velocity field formed between two fluid streams of different density and/or viscosity which is described by Equations 120 through 122 was investigated by Lock (1951) [10] and Kenlegan (1944) [7]. We shall employ the results of the former since the latter's analysis assumes an approximate expression for the boundary layer thickness is not general and is developed only for the case where one of the fluid streams is at rest. The results obtained from a numerical solution of Equation 120 through 122 by the method developed by Lock for the case of $\Lambda = 1/2$,

1, 3 and $\Lambda = 1.0$ are given in Tables 1, 2 and 3. Note that the mixing layer thickness of the suspension is smaller than that of the clean fluid, and that the interface velocity increases as Λ increases. Equations 114 and 115 can be written as:

$$h_4(\eta^*) = \frac{1}{2} F_o F_o'' \tag{123}$$

$$\frac{g_5(\eta^*)}{\Gamma(\Lambda+1)^{1/4}} = -\frac{1}{2} F_o (F_o'')^{3/2} \tag{124}$$

The significant feature to observe here is that the slip velocities are proportional to the local flow acceleration, 1/2 Fo Fo". These results are quite reasonable since we would expect the particulate phase velocity for $\xi >> 1$ to be independent of previous history of motion, and governed by the local flow conditions. Moreover, the slip velocity transverse to the main direction of motion is proportional to the local shear gradient. This is in sharp contrast to the results obtained in the case of $\xi << 1$, where the particulate phase motion was determined by the initial conditions and by the integrated history of the motion. Finally, it is worthwhile to note that this type of general behavior was predicted by Marble in reference 12.

Recall that the zeroth order solution represents the case in which the two phases move as one phase, i.e., the particles are frozen to the surrounding fluid. Consequently, the particulate phase to the zeroth order has a velocity in the normal direction given by:

$$v_p^{*(0)} = \xi^{-1/2} \frac{1}{2} (\eta^* F_o' - F_o) \tag{125}$$

Note that the effect of this velocity is to transport the particulate phase from the mixing layer into the main portion of the suspension stream. Graphical representation of Equations 123 through 125 for the case where $\Lambda = 1$ and $\lambda = 1/2$ or 3 are given in Figures 7 through 9. Observe that the slip shear forces result in a migration of the particles towards the interface of the two streams. However, because $g_5(0) = 0$, migration of particles across this interface does not occur.

The particulate phase density distribution is determined by Equation 107 which after substitution of Equations 107 through 111 yields:

$$f_o K_3' + \frac{3}{2} f_o' K_3 = 2 g_5'(\eta)$$

which can be written as:

$$F_o K_3' + \frac{3}{2} F_o' K_3 = 2 g_5' (\overset{*}{\eta}) \tag{126}$$

and which after integration becomes:

$$K_3(\overset{*}{\eta}) = \frac{2 \int_o^{\overset{*}{\eta}} F_o^{1/2}(x)\, g_5'(x)\, dx}{\left[F_o(\overset{*}{\eta}) \right]^{3/2}} \tag{127}$$

Note that the latter is determined not only by the local flow field, but also by and integrated effect of the lateral slip velocity gradient. In addition we can show that,

$$\lim_{\overset{*}{\eta} \to o} K_3(\overset{*}{\eta}) = \frac{4}{3} \frac{g_5'(o)}{F_o'(o)} \tag{128}$$

Figure 10 gives $K_3(\overset{*}{\eta})$ as determined by numerical integration of Equation 127 for the case where $\Lambda = 1$ and $\lambda = 1/2$, 3. Before interpre-

tating this curve recall that:

$$\frac{\partial \rho_p^*}{\partial x} = \frac{\partial \rho_p^*}{\partial \xi} - \frac{\eta}{2\xi}\frac{\partial \rho_p^*}{\partial \eta}$$

Therefore, to the first order,

$$\frac{\partial \rho_p^{*(1)}}{\partial x^*} = -\frac{3}{4}\xi^{-7/4} K_3(\eta) - \frac{\eta}{2}\xi^{-7/4} K_3'(\eta) \qquad (129)$$

Since K_3 is negative at $\eta = 0$, the particulate phase tends to accumulate along the interface. Moreover, near the edge of mixing layer where $K_3'(\eta) = 0$, the particulate phase density is diminished as a result of being convected out of the mixing zone.

The next higher order modification of the particulate phase density $K_4(\eta^*)$ is due to drag effects and is determined by:

$$F_0 K_4' + 2F_0' K_4 = 2\left(g_c'(\eta) - h_4 - \frac{\eta^*}{2} h_4'\right) \qquad (130)$$

which after simplification becomes:

$$d\left(K_4 F_0^2\right) = F_0 F_0''\left(\eta^* F_0' - F_0\right) d\eta^*$$

Since, $F_0(0) = 0$,

$$K_4(\eta^*) = \frac{\int_0^{\eta^*} F_0(x) F_0''(x)\left(x F_0' - F_0\right) dx}{\left[F_0(\eta^*)\right]^2} \qquad (131)$$

It can be shown that:

$$\lim_{\eta^* \to 0} K_4(\eta^*) = \frac{1}{2} \lim_{\eta^* \to 0} \frac{F_0''\left(\eta F_0' - F_0\right)}{F_0} \qquad (132)$$

$$= 0$$

A plot of $K_4(\overset{*}{\eta})$ is shown in Figure 11.

Finally, the first order modification $F_3'(\overset{*}{\eta})$ to the fluid velocity is determined by:

$$F_3''' + \frac{1}{(\Lambda+1)^{1/2}}\left\{\tfrac{1}{2}F_0F_3'' + \tfrac{3}{4}F_0'F_3' - \tfrac{1}{4}F_0''F_3\right\} = -\frac{\Lambda}{(\Lambda+1)}I(\overset{*}{\eta}) \tag{133}$$

where

$$I(\overset{*}{\eta}) = K_3(\overset{*}{\eta})\,h_4(\overset{*}{\eta}) \tag{134}$$

which is valid for the region $(\xi, \eta \geq 0)$ and

$$g_3''' + \frac{1}{2}g_0g_3'' + \frac{3}{4}g_0'g_3' - \frac{1}{4}g_0''g_3 = 0 \tag{135}$$

which is valid in the region $(\xi, \eta \leq 0)$.

The connected boundary conditions for Equations 133 and 135 are:

$$\begin{aligned} F_3'(\infty) &= g_3'(-\infty) \\ F_3(0) &= g_3(0) = 0 \\ F_3'(0) &= g_3'(0) \\ (\Lambda+1)^{1/2}F_3''(0) &= g_3''(0) \end{aligned} \tag{136}$$

It is evident, that there are a double infinity of solutions for Equation 133 through 136 depending on the parameters Λ and Λ. Because for given values of these parameters it is not easy to find the appropriate solution, a numerical solution has up to date not been obtained. Similar difficulties were reported by Singleton [16]. We do not persue this

matter further since we are primarily interested in particle migration characteristics and because the latter are not significantly effected by the first order modification of the fluid phase velocity field. Techniques for calculating the latter in regions of small slip represent a sufficiently important problem to merit further investigation on its own.

Summary and Discussion:

An analysis of laminar mixing of a suspension stream with a clean fluid stream which included the effects of both drag and slip-shear forces was performed. It was shown that the former determine the interaction between the phases and the particulate velocity distribution in the main flow direction while the latter primarily determine the particulate density field and the particle migrations in the direction normal to the main flow. It was shown that injection of the particulate into the clean fluid region is due entirely to the effects of the slip-shear forces. Moreover, that this injection occurs only within "leading edge" portion of the mixing region where $\xi << 1$. In this region particles exhibit two-directional migration characteristics, where in general the particles near the interface tend to move towards the clean fluid, while those close to the edge of the boundary layer move into the undisturbed suspension stream. Equation 91 gives the vertical position within the mixing layer at which the transverse velocity of the particles is zero, i.e., the particles are moving only in the main flow direction. This position is a function of Γ, the slip-shear parameter.

In the far downstream region where $\xi >> 1$, the slip between the phases is small and injection of the particulate from the suspension

into the lower stream does not occur. However, the first order modification to the particle phase bulk transport velocity in the normal direction is again due to slip-shear effects. Furthermore, in this regime the slip velocities are proportional to the local flow acceleration. This is in sharp contrast to the results obtained for the case of $\xi \ll 1$, where the particulate phase motion was determined by the initial conditions and by integrated effect the drag forces.

We have determined for the initial and far out mixing regions the growth of the mixing layer, the velocity field of the phases, and the number of particles per unit volume. Unfortunately, direct comparison of these results with experimental findings is impossible, due to the unavailability of the latter. However, in this connection, consider a series of experiments reported by Karmis, et. al. [6] in which a suspension was pumped through a tube. It was observed that in those cases where the solid phase lagged the fluid, a particle free zone developed near the wall. During these experiments, the Saffman [14] condition of $(Re)_k/(Re)_p^2 >> 1$ was not strictly fulfilled. The latter varied between 10 and 100 for runs in which the free particle zone was observed. However, in spite of this, it would appear reasonable in light of our theoretical findings, that the particle free zone was caused by the combined effects of the inertial wall effect and the slip-shear forces which acted on the particles to move them towards the centerline. In cases where the particles lead the fluid, the slip-shear forces would tend to move the particles towards the walls of the tube. This indeed was the case for particles located near the center of the tube. However, particles very close to the wall migrated away from it. In addition, Young [21], in similar experiments (and for the case where the particles

lead the fluid) reported migration towards and particle accumulation at the walls. Serge and Silberberg [15] performed experiments on dilute suspensions of neutrally buoyant spheres and observed that the particles migrated to an equilibrium position approximately half way between the wall and axis of the tube. Where the two-directional migration consisted of particles near the wall moving inward, while those near the axis moved outward.

Recall that the herein predicted two-directional migration of particles within the suspension stream resulted from the opposing effects (in the transverse direction) of drag and slip-shear forces. However, because the vertical component of fluid velocity for tube flow is zero, transport of particles in the radial direction by means of drag forces does not occur. Consequently, the phenomena observed by Serge and Silberberg probably have resulted from the opposing effects of slip-shear and wall forces.

Finally note that the problem of mixing of two streams presents a unique opportunity to experimentally investigate the boundary layer flow of a suspension in the absence of the wall effects, as such it represents an ideally suited problem for investigation of the drag, lift, slip-shear caused particle migrations.

Acknowledgment:

The authors would like to express their sincere appreciation to the National Science Foundation for its generous support which has helped make this investigation possible.

NOTATION

a = particle radius

D = drag force acting on particle

$f_{(i)}(\eta)$ = coefficient in expansion of dimensionless fluid stream function

$g_{(i)}(\eta)$ = coefficient in expansion of dimensionless particulate slip velocity in the y-direction

$h_{(i)}(\eta)$ = coefficient in expansion of dimensionless particulate stream function, or coefficient in expansion of dimensionless particulate slip velocity in the x-direction

k = absolute value of velocity gradient

$K_{(i)}(\eta)$ = coefficient in expansion of dimensionless particulate phase density function

L = transverse force acting on particle

P = fluid pressure

$g_{(i)}(\eta)$ = coefficient in expansion of dimensionless fluid stream function

(R_e) = particle Reynolds number

t = time

u, v = Cartesian velocity components

x, y = Cartesian coordinates

X_p = force per unit volume exerted by particle on fluid

$\xi = x/\lambda$ = dimensionless transform coordinate in the flow direction

$\eta = \overset{*}{y}/(\overset{*}{x})^{1/2}$ = dimensionless transform coordinate normal to the flow direction

$\overset{*}{\eta} = \eta(A+1)^{1/2}$ = modified dimensionless transform coordinate normal to the flow direction

ϕ = dimensionless time

λ = slip relaxation length for particulate phase

μ = fluid viscosity

ν = kinematic viscosity of fluid

ρ = mass density

τ_p = slip relaxation time for particulate phase

$\psi(\xi,\eta)$ = boundary layer stream function

Ω = angular velocity of particle

Subscripts

k = fluid shear effect

p = particle

s = solid, also slip

Ω = rotation effect

Superscripts

$*$ = dimensionless

$-$ = average

Parametric Group

$A = \rho_p/\rho$ = particle density ratio at reference state

$\Lambda = (u_1-u_2)/(u_1+u_2)$ = average velocity difference between the two mixing streams

$\Gamma = 4.5\left(\frac{\rho}{\rho_s}\right)^{1/2}\left(\frac{\bar{u}\lambda}{\nu}\right)^{3/4}$ = particle parameter associated with slip-sheat effects

Bibliography

1. Brenner, Howard, "Advances in Chemical Engineering, Vol. 6" Academic Press. (1966)

2. Carrier, G.F., "Shock Waves in a Dusty Gas," J. Fluid Mechanics, Vol. 4 (1958), pp. 376-382.

3. Chiu, H.H., "Boundary Layer Flow with Suspended Particles," Princeton University, Report 620 (August 1962).

4. Gortler, H., "Brechnung von Aufgaben der Freim Turbulenz," Zeitschrift Angewandte Mathematik und Mechanik, Bd. 22, No. 5 (1942).

5. Hinze, J.O., "Momentum and Mechanical Energy Balance Equations for a Flowing Homogeneous Suspension,"Applied Science Research, Vol. 11, (1962), Section A, pg. 33.

6. Karmis, A., Goldsmith, H.L., and Mason, S.G., "The Flow of Suspensions through Tubes," Can. J. of Chem. Eng., (1966), pp. 181-193.

7. Keulegan, G.H., "Laminar Flow at the Interface of Two Liquids," Jour. of Research N.B. Standards, Vol. 32, (1944) pg. 303-327.

8. Lawler, M.T. and Lu, P.C., "A Study of Radical Migrations in Fluid-Particle Flows with Fluid Rorations," Report FTAS/TR-67-27, Case Western Reserve University (1967).

9. Liu, J.T.C., "On Hydrodynamic Stability of Parallel Dusty Gas Flows," Physics of Fluids, Vol. 8 (1965), pg. 1939.

10. Lock, R.C., "The Velocity Distribution in the Laminar Boundary Layer Between Parallel Streams," Quart. Journal Mech. and Applied Meth. Vol. IV, Pt. 11 (1951).

11. Marble, Frank E., "Dynamics of a Gas Containing Small Solid Particles," presented at the Fifth AGARD Combustion and Propulsion Colloquium, Braunschweig (April, 1962).

12. Otterman, Bernard, "Laminar Boundary Layer Flows of a Two-Phase Suspension," Ph.D. Thesis, State University of N.Y. at Stony Brook (1968).

13. Rubinow, S.I. AND Keller, Joseph B., "The Transverse Force on a Spinning Sphere Moving in a Viscous Fluid," Journal of Fluid Mechanics, Vol. II (1961), pp. 447-459.

14. Saffman, P.G., "The Lift on a Small Sphere in a Slow Shear Flow," J. Fluid Mechanics (1965), Vol. 22, Part 2, pp. 385-400.

15. Segre, G. and Silberberg, A., "Behavior of Macroscopic Rigid Spheres in Poiseville Flow," Journal of Fluid Mechanics, Vol. 14 (1962), pp. 115-157.

16. Singleton, Robert E., "Compressible Gas-Solid Particle Flow Over a Semi-Infinite Flat Plate," ZAMP, Vol. 16 (1965), pp. 421-448.

17. Singleton, Robert E., "Fluid Mechanics of Gas-Solid Particle Flow in Boundary Layers," Ph.D. Thesis, C.I.T., 1964.

18. Soo, S.L., "Fluid Dynamics of Multiphase Systems," Blaisdell Pub. Co., Waltham, Massachusetts (1967).

19. Soo, S.L., "Laminar and Separated Flow of a Particulate Suspension," Astronautica Acta, Vol. 11, No. 6, 1965.

20. Torobin, L.B. and Gauvin, W.H., "Fundamental Aspects of Solid-Gas Flow," Canadian J. of Chem. Eng., (in 5 parts), Vol. 37, pp. 129, 167, 224 (1959) and Vol. 38, pp. 142, 189 (1960).

21. Young, D.F., A.S.M.E. paper No. 60 - HYD-12, 1960.

Table I

Solution of Equations 120 through 122 for the Case of $\Lambda=1$, $s=1/2$

η^*	$F_o(\eta^*)$	$F_o'(\eta^*)$	$F_o''(\eta^*)$
0.0000	0.0000	1.1300	0.5886
0.2000	0.1658	1.2131	0.5851
0.4000	0.3430	1.2951	0.5747
0.6000	0.5319	1.3753	0.5573
0.8000	0.7320	1.4523	0.5330
1.0000	0.9427	1.5255	0.5023
1.2000	1.1633	1.5943	0.4664
1.4000	1.3934	1.6572	0.4260
1.6000	1.6319	1.7145	0.3827
1.8000	1.8780	1.7654	0.3383
2.0000	2.1310	1.8101	0.2934
2.2000	2.3839	1.8485	0.2502
2.4000	2.6536	1.8809	0.2095
2.6000	2.9216	1.9080	0.1719
2.8000	3.1931	1.9299	0.1383
3.0000	3.4673	1.9472	0.1096
3.2000	3.7436	1.9610	0.0848
3.4000	4.0218	1.9714	0.0645
3.6000	4.3012	1.9792	0.0482
3.8000	4.5816	1.9853	0.0352
4.0000	4.8627	1.9894	0.0252
4.2000	5.1443	1.9923	0.0177
4.4000	5.4262	1.9945	0.0122
4.6000	5.7083	1.9958	0.0083
4.8000	5.9907	1.9968	0.0053
5.0000	6.2732	1.9975	0.0036

Table 2

Solution of Equations 120 through 122 for Case of $\Lambda=1$, $s=1$

$\overset{*}{\eta}$	$F_o(\overset{*}{\eta})$	$F_o'(\overset{*}{\eta})$	$F_o''(\overset{*}{\eta})$
0.0000	0.0000	1.0971	0.6067
0.2000	0.1613	1.1828	0.6033
0.4000	0.3345	1.2673	0.5929
0.6000	0.5194	1.3501	0.5751
0.8000	0.7161	1.4297	0.5506
1.0000	0.9236	1.5054	0.5197
1.2000	1.1414	0.5764	0.4833
1.4000	1.3691	1.6416	0.4422
1.6000	1.6055	1.7011	0.3981
1.8000	1.8498	1.7542	0.3522
2.0000	2.1012	1.8008	0.3064
2.2000	2.3588	1.8409	0.2617
2.4000	2.6215	1.8749	0.2196
2.6000	2.8886	1.9032	0.1806
2.8000	3.1594	1.9262	0.1458
3.0000	3.4331	1.9445	0.1156
3.2000	3.7091	1.9589	0.0897
3.4000	3.9869	1.9701	0.0684
3.6000	4.2660	1.9784	0.0509
3.8000	4.5463	1.9847	0.0373
4.0000	4.8272	1.9891	0.0267
4.2000	5.1087	1.9925	0.0191
4.4000	5.3905	1.9947	0.0128
4.6000	5.6727	1.9962	0.0086
4.8000	5.9550	1.9972	0.0059
5.0000	6.2375	1.9978	0.0040

Table 3

Solution of Equations 120 through 122 for the case of $\Lambda=1$, $s=3$

η^*	$F_o(\eta^*)$	$F_o'(\eta^*)$	$F_o''(\eta^*)$
0.0000	0.0000	1.0198	0.6477
0.2000	0.1506	1.1113	0.6443
0.4000	0.3141	1.2018	0.6339
0.6000	0.4904	1.2902	0.6162
0.8000	0.6788	1.3756	0.5913
1.0000	0.8792	1.4572	0.5597
1.2000	1.0907	1.5336	0.5221
1.4000	1.3126	1.6046	0.4795
1.6000	1.5441	1.6691	0.4335
1.8000	1.7843	1.7270	0.3852
2.0000	2.0322	1.7780	0.3365
2.2000	2.2867	1.8222	0.2891
2.4000	2.5471	1.8601	0.2435
2.6000	2.8124	1.8915	0.2016
2.8000	3.0817	1.9173	0.1638
3.0000	3.3543	1.9379	0.1302
3.2000	3.6296	1.9544	0.1017
3.4000	3.9068	1.9669	0.0782
3.6000	4.1857	1.9766	0.0585
3.8000	4.4656	1.9837	0.0430
4.0000	4.7464	1.9890	0.0310
4.2000	5.0280	1.9928	0.0223
4.4000	5.3099	1.9954	0.0153
4.6000	5.5922	1.9970	0.0103
4.8000	5.8745	1.9982	0.0069
5.0000	6.1571	1.9990	0.0046

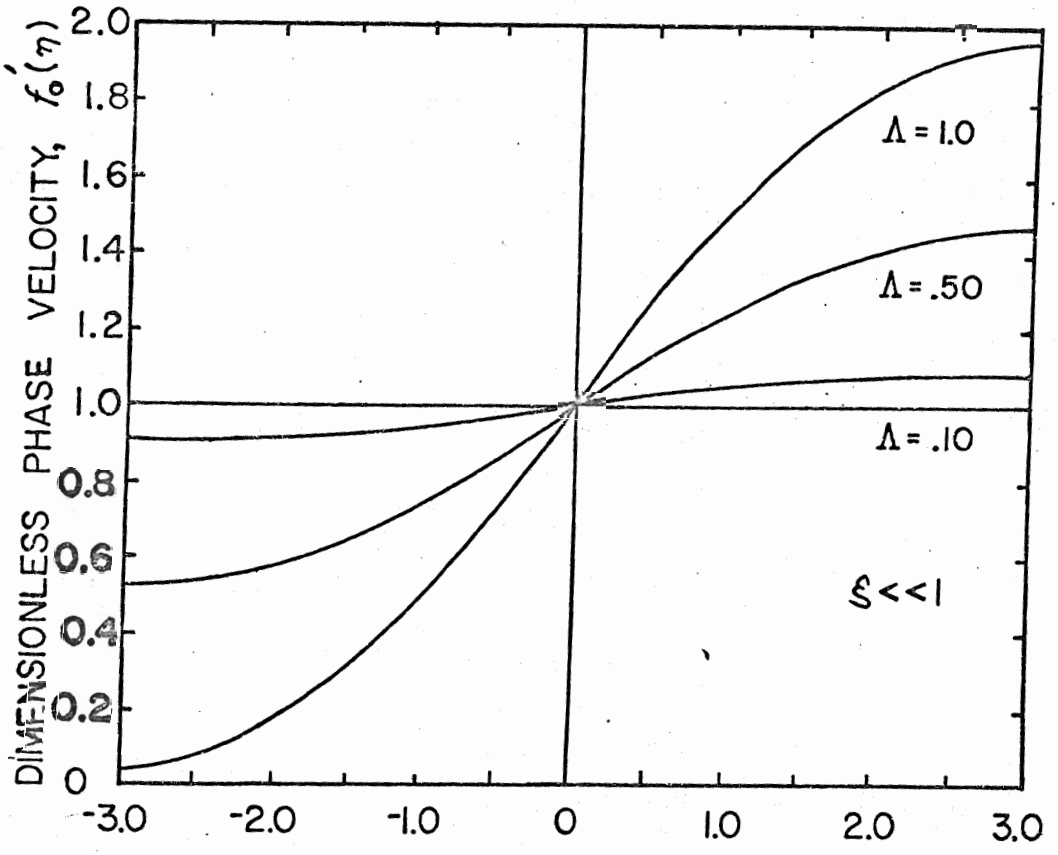

FIG. 1 FLUID PHASE VELOCITY, $f_o'(\eta)$, FOR THE CASE OF LARGE SLIP, $\xi << 1$.

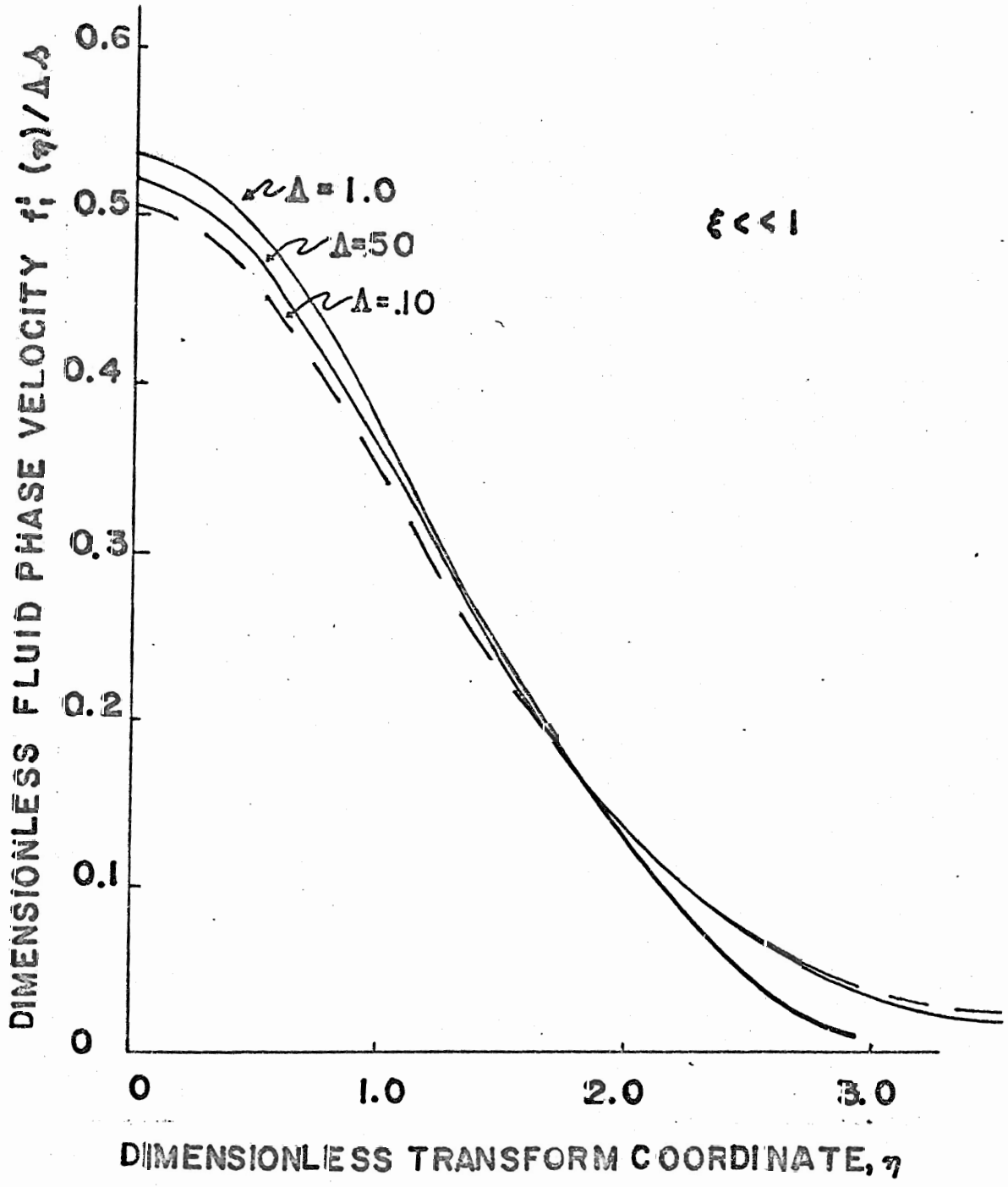

FIG. 2 FLUID PHASE VELOCITY, $f_1'(\eta)$

FOR THE CASE OF $\xi << 1$

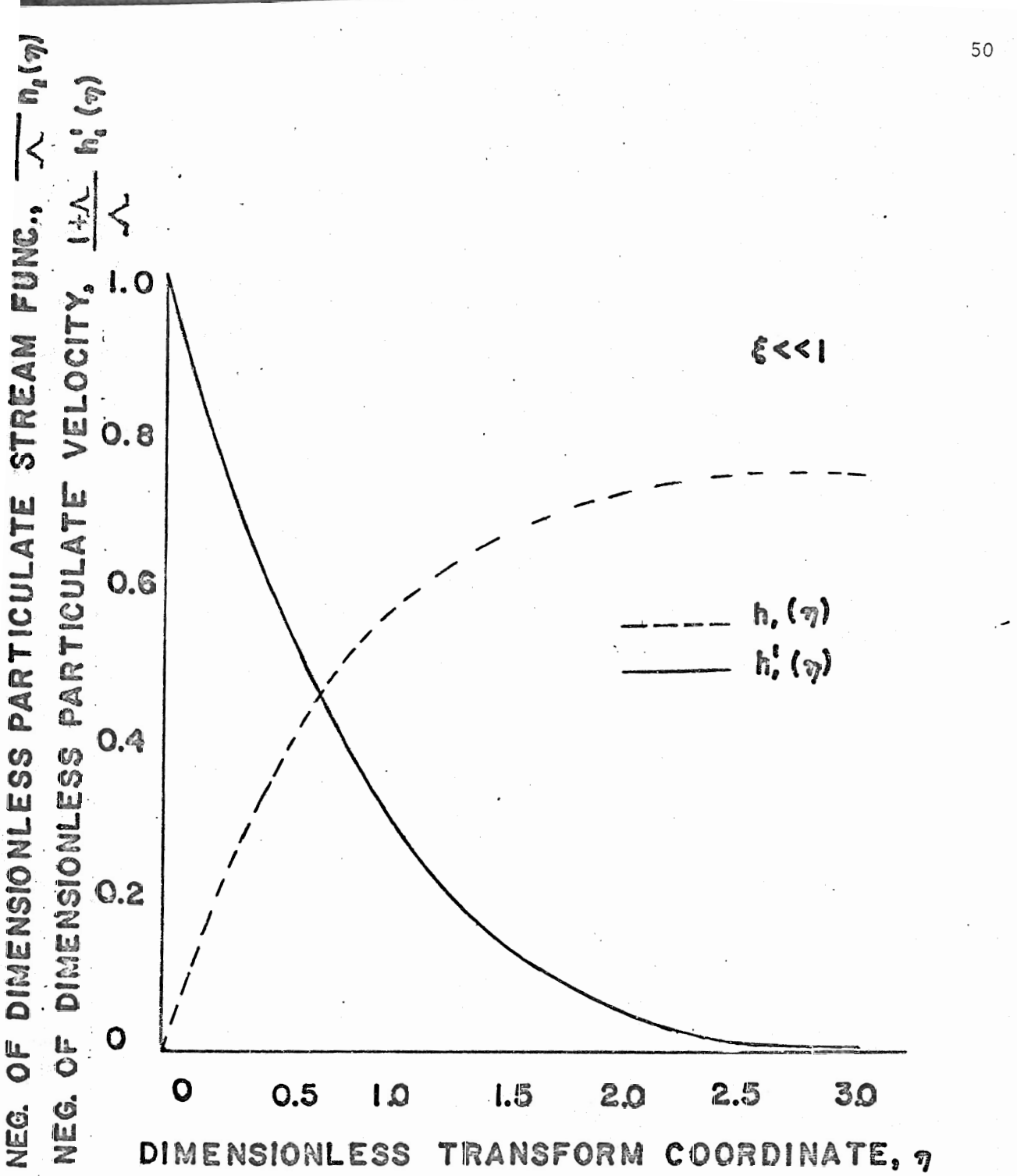

FIG. 3 PARTICULATE STREAM FUNCTION $h_1(\eta)$, AND VELOCITY $h_1'(\eta)$ FOR $\epsilon << 1$

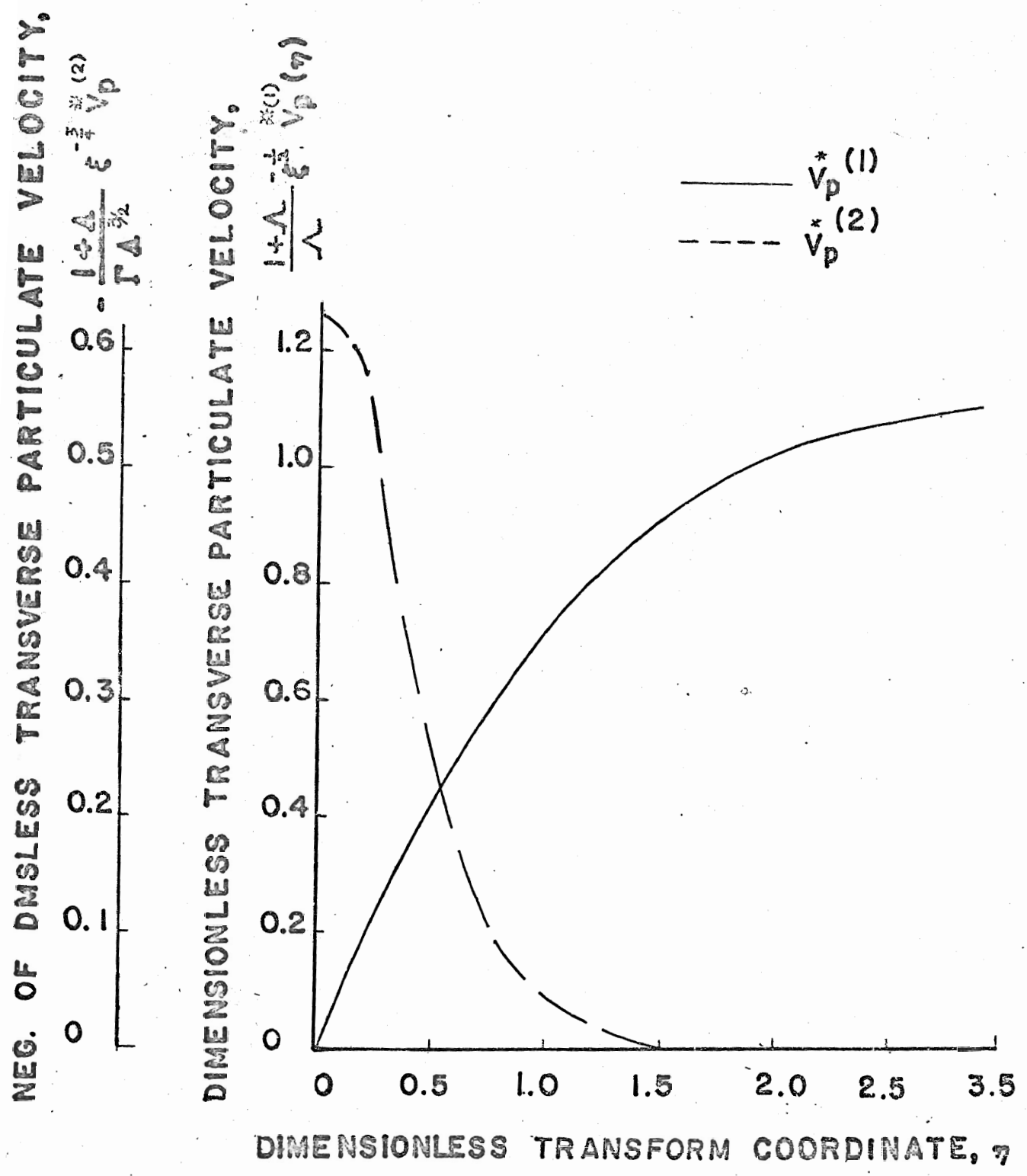

FIG. 4 PARTICULATE VELOCITY, $V_p^{*(1)}(\eta)$, AND $V_p^{*(2)}$ FOR $\xi \ll 1$

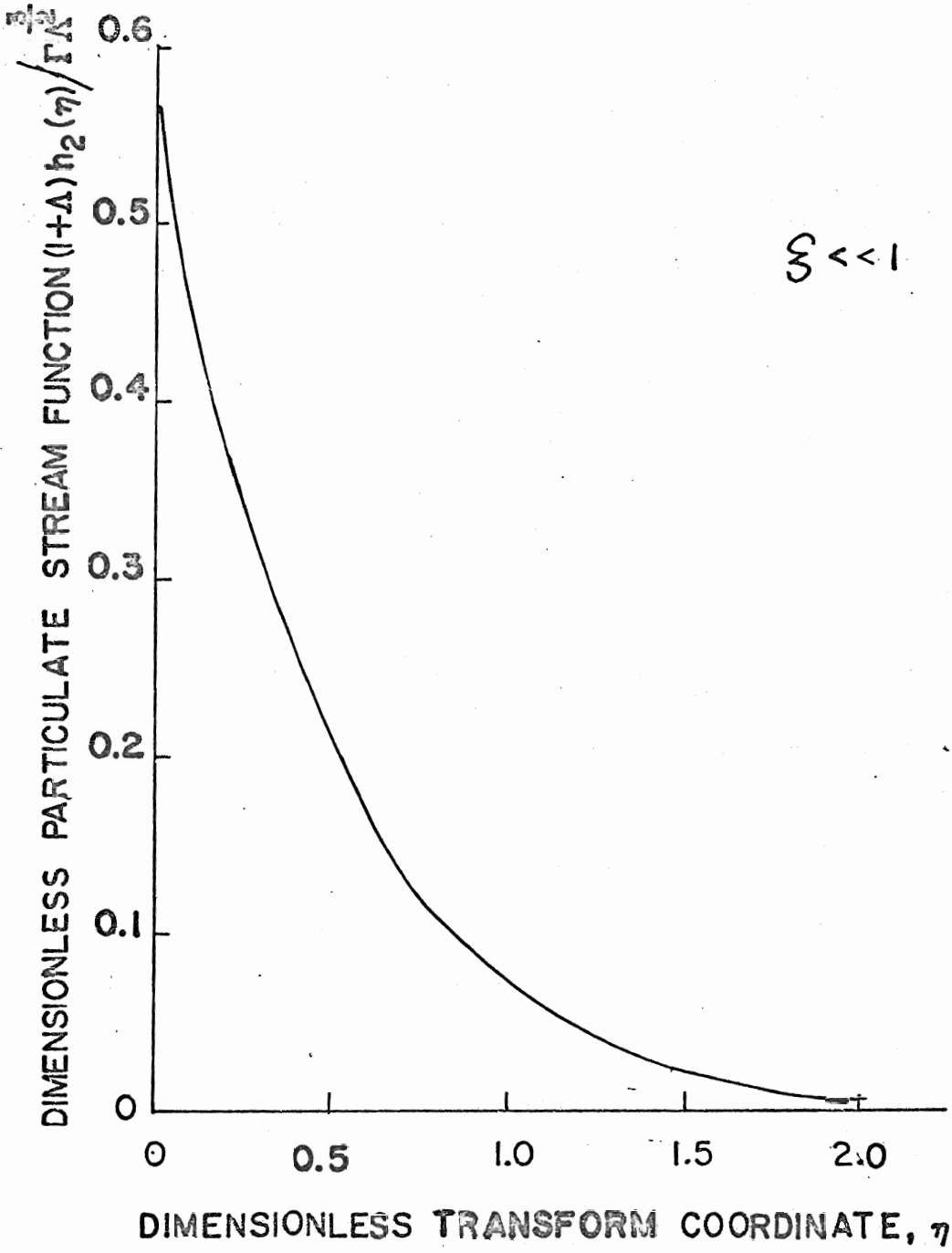

FIG. 5 PARTICULATE STREAM FUNCTION $h_2(\eta)$, FOR THE CASE OF $\xi << 1$

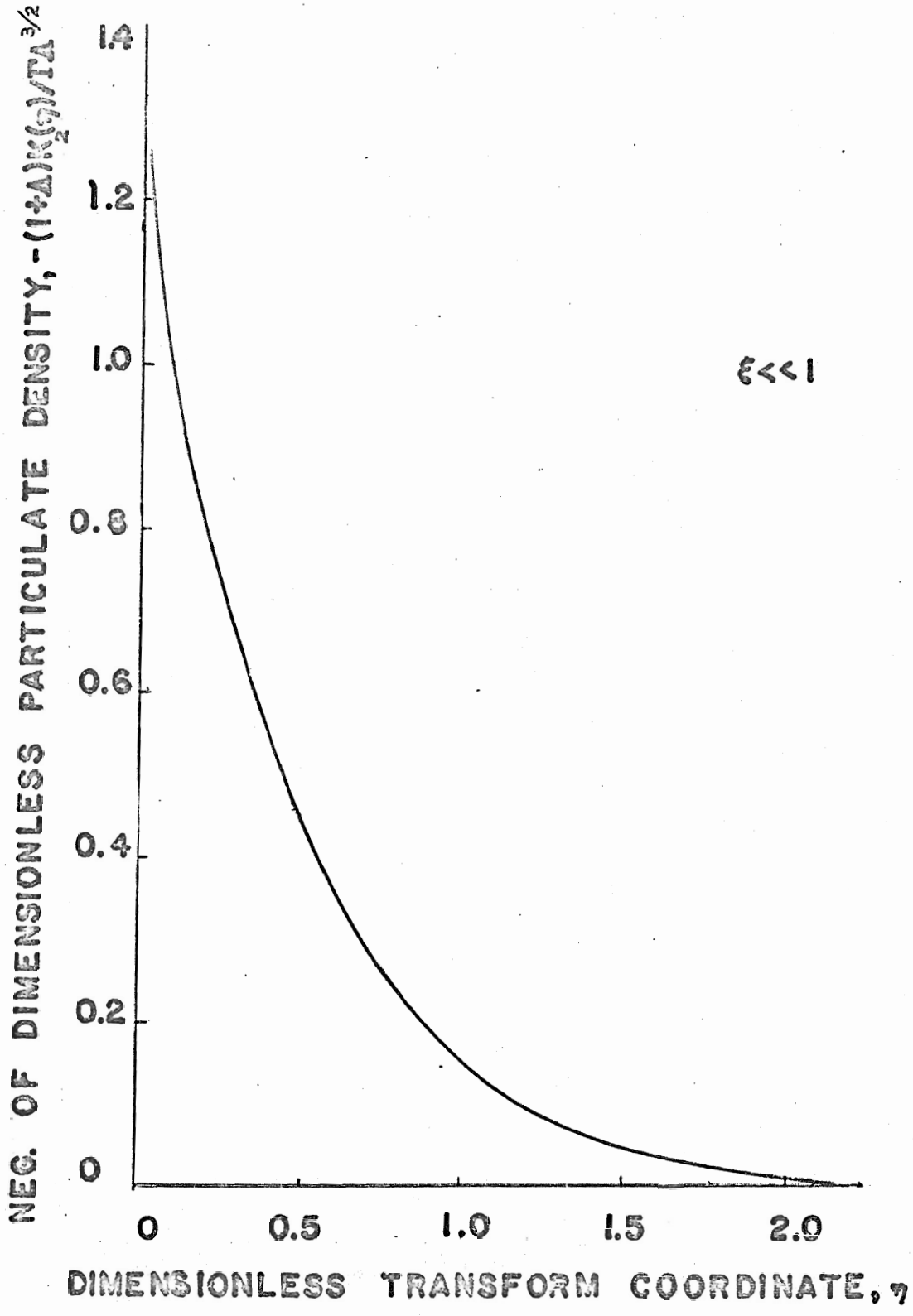

FIG. 6 PARTICULATE DENSITY $K_2(\eta)$, FOR THE CASE OF $\xi<<1$

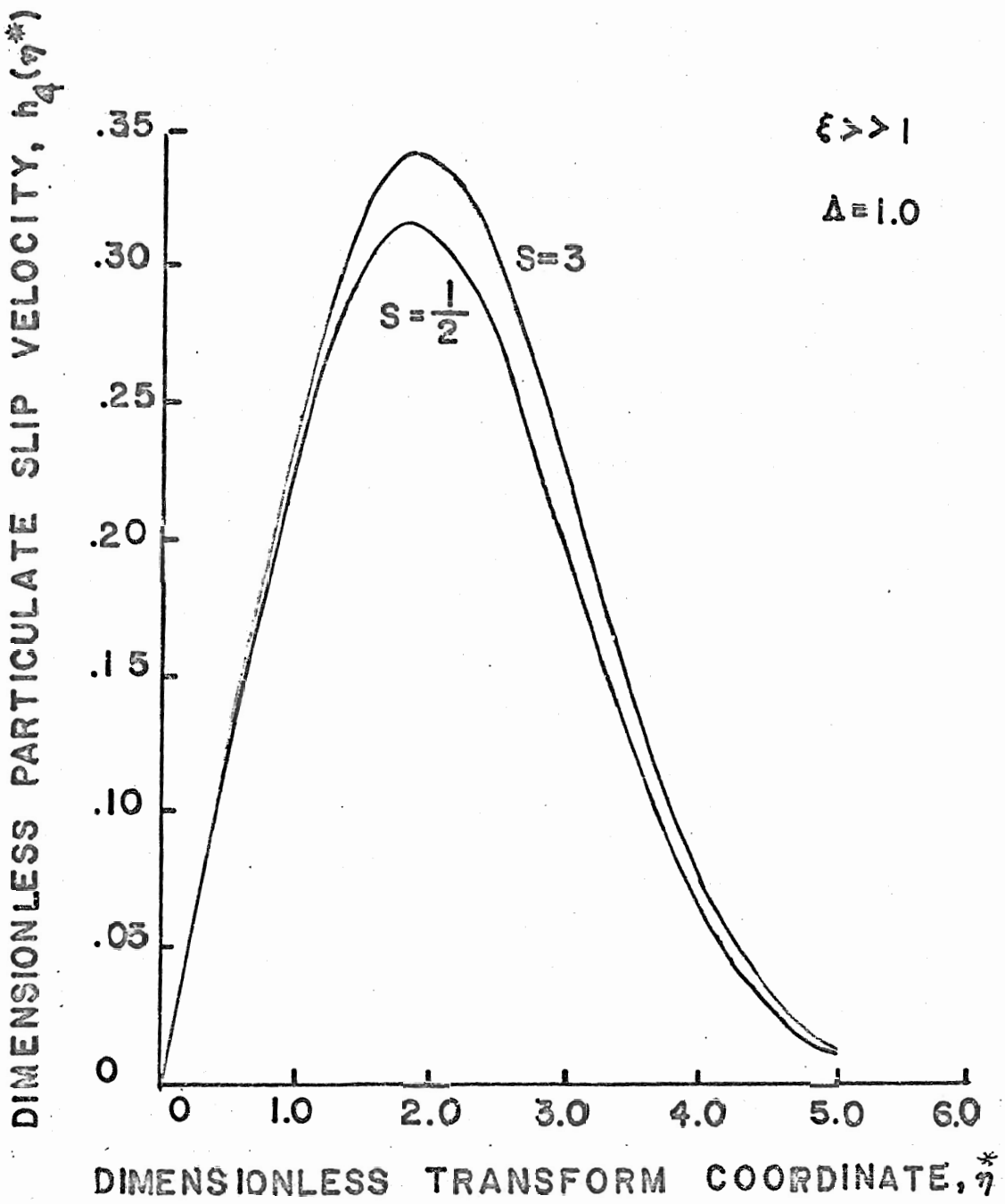

FIG. 7 FIRST ORDER PARTICULATE SLIP VELOCITY IN CASE OF $\xi >> 1$

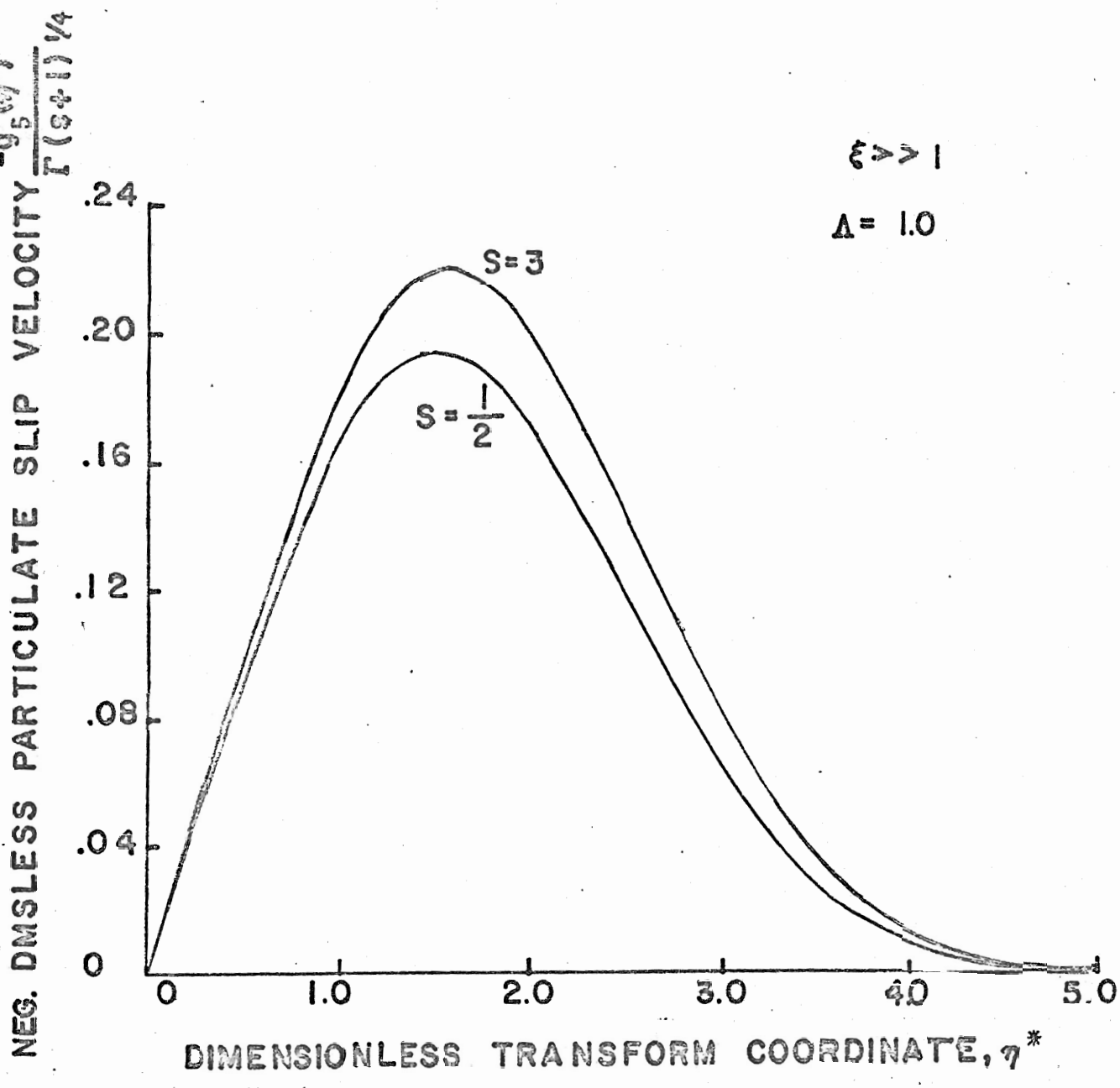

FIG. 8 PARTICULATE SLIP VELOCITY, $g_5(\eta^*)$, IN CASE OF SMALL SLIP, $\xi >> 1$

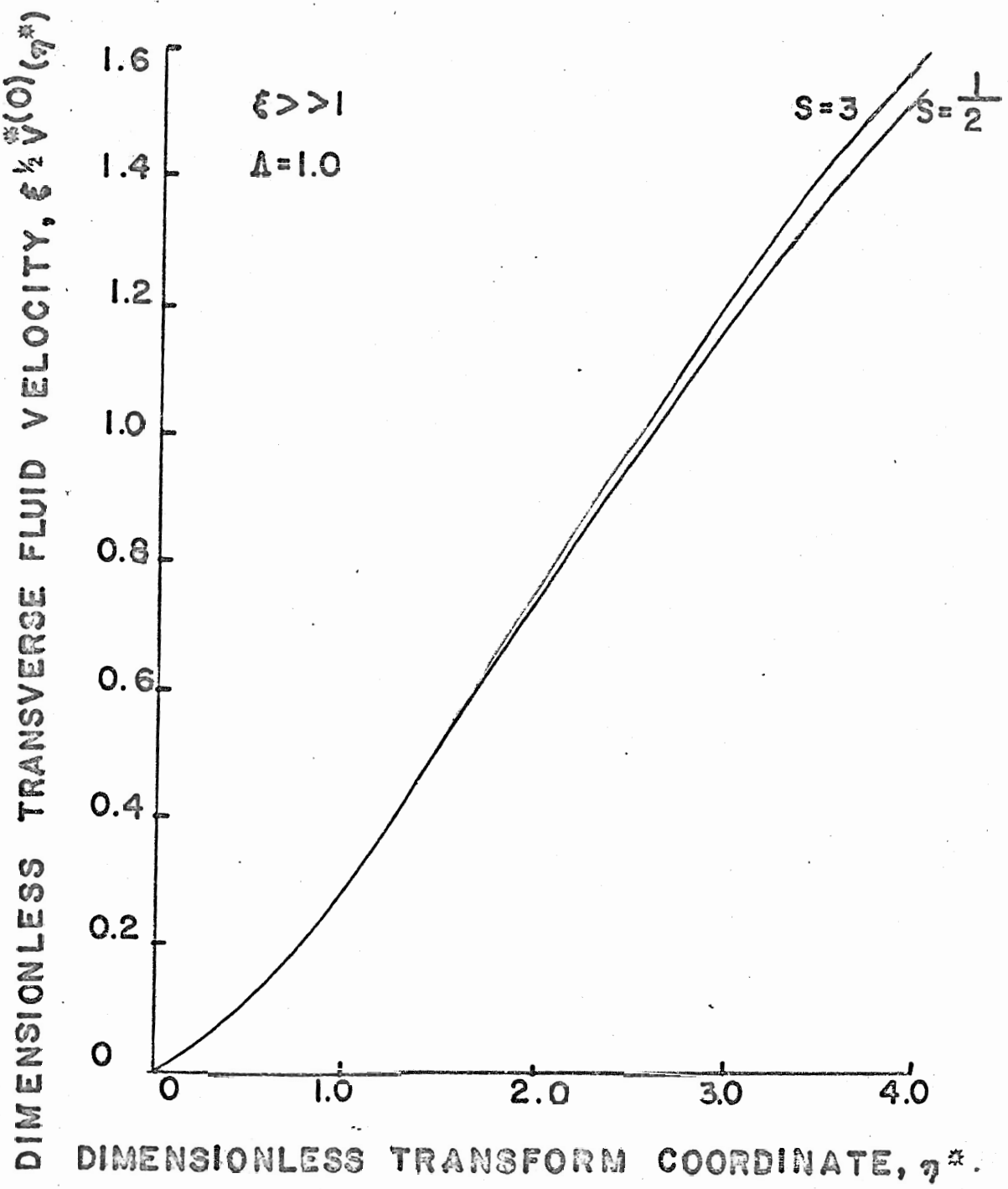

FIG. 9 TRANSVERSE FLUID VELOCITY IN THE CASE OF SMALL SLIP, $\xi >> 1$

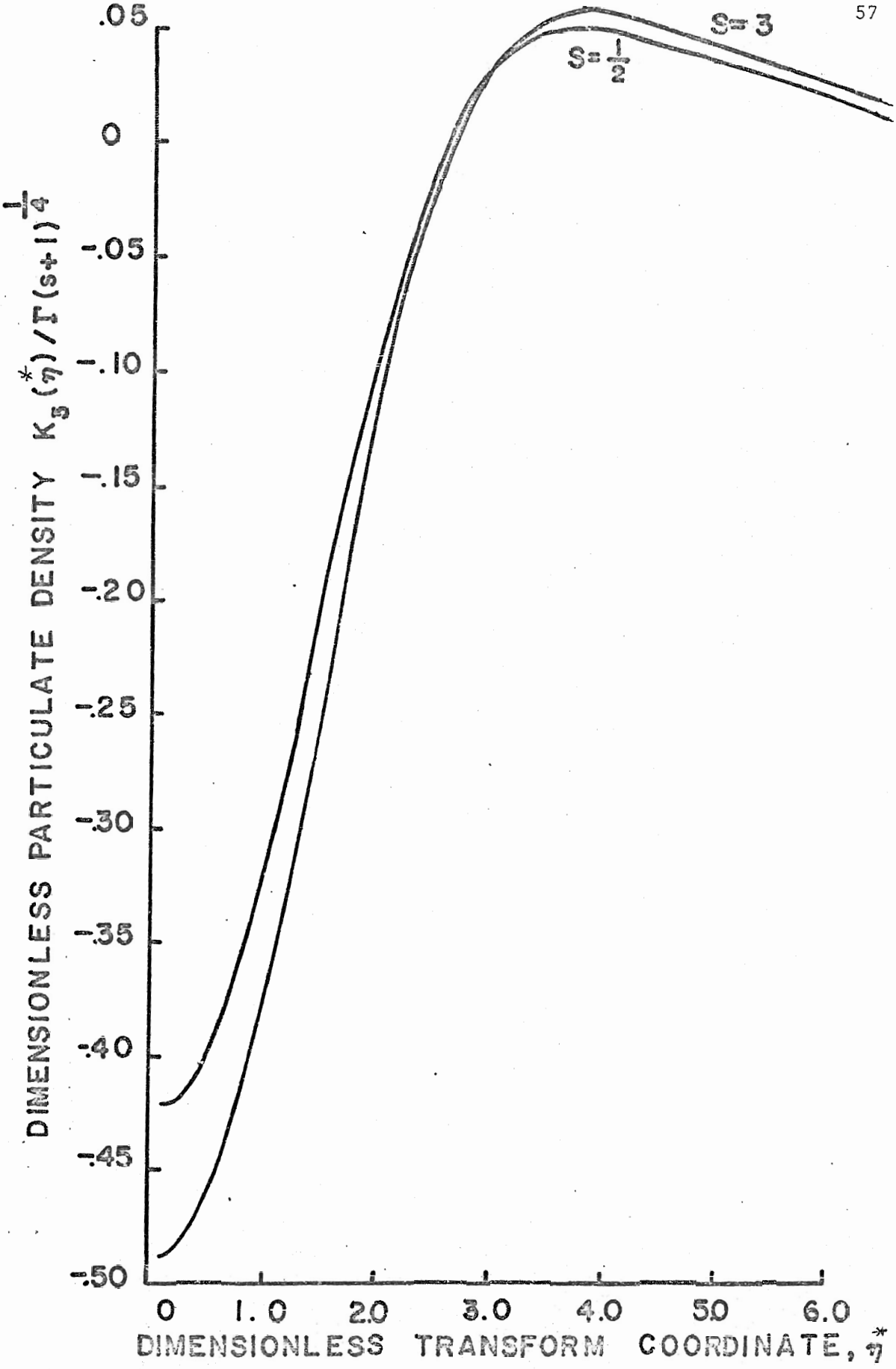

FIG. 10 PARTICULATE DENSITY $K_3(\eta^*)$

FOR THE CASE OF $\xi >> 1$

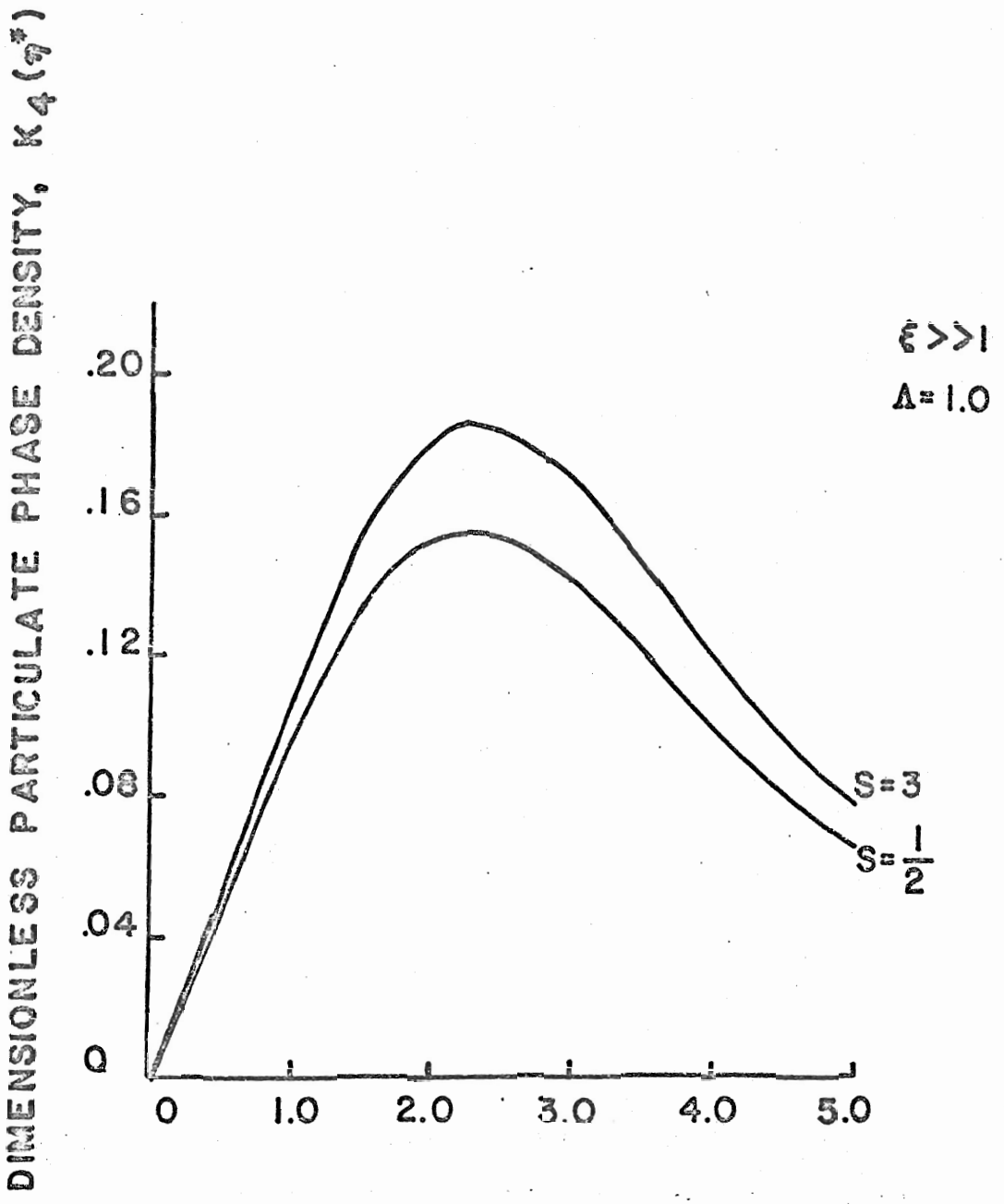

FIG. II PARTICULATE DENSITY $K_4(\eta^*)$, FOR THE CASE OF $\xi >> 1$